



**HAL**  
open science

## **PIKfyve activity regulates reformation of terminal storage lysosomes from endolysosomes**

Christin Bissig, Pauline Croise, Xavier Heiligenstein, Ilse Hurbain, Guy M Lenk, Emily Kaufman, Ragna Sannerud, Wim Annaert, Miriam H. Meisler, Lois S. Weisman, et al.

### ► **To cite this version:**

Christin Bissig, Pauline Croise, Xavier Heiligenstein, Ilse Hurbain, Guy M Lenk, et al.. PIKfyve activity regulates reformation of terminal storage lysosomes from endolysosomes. *Traffic*, 2017, 18 (11), pp.747-757. 10.1111/tra.12525 . hal-02359729

**HAL Id: hal-02359729**

**<https://hal.science/hal-02359729>**

Submitted on 5 Dec 2019

**HAL** is a multi-disciplinary open access archive for the deposit and dissemination of scientific research documents, whether they are published or not. The documents may come from teaching and research institutions in France or abroad, or from public or private research centers.

L'archive ouverte pluridisciplinaire **HAL**, est destinée au dépôt et à la diffusion de documents scientifiques de niveau recherche, publiés ou non, émanant des établissements d'enseignement et de recherche français ou étrangers, des laboratoires publics ou privés.

## **PIKfyve complex regulates early melanosome homeostasis required for physiological amyloid formation**

Christin Bissig<sup>1</sup>, Pauline Croisé<sup>2</sup>, Xavier Heiligenstein<sup>1,3</sup>, Ilse Hurbain<sup>1,3</sup>, Guy M. Lenk<sup>4</sup>, Emily Kaufman<sup>5</sup>, Ragna Sannerud<sup>6,7</sup>, Wim Annaert<sup>6,7</sup>, Miriam H. Meisler<sup>4</sup>, Lois S. Weisman<sup>5</sup>, Graça Raposo<sup>1,3</sup> and Guillaume van Niel<sup>1,2,3</sup>

1. Structure and Membrane Compartments, Institut Curie, Paris Sciences & Lettres Research University, Centre National de la Recherche Scientifique, UMR144, Paris, France
2. IPNP, Institute of Psychiatry and Neuroscience of Paris, Hopital Saint-Anne, Université Paris Descartes, INSERM U894, Paris, France
3. Cell and Tissue Imaging Facility, Institut Curie, Paris Sciences & Lettres Research University, Centre National de la Recherche Scientifique, UMR144, Paris, France.
4. Department of Human Genetics, University of Michigan, Ann Arbor, Michigan, USA
5. Life Science Institute, University of Michigan, Ann Arbor, Michigan, USA
7. VIB Center for Brain & Disease Research, Leuven, Belgium
8. KU Leuven, Department of Neurosciences, Leuven, Belgium

Corresponding author: Guillaume van Niel, [guillaume.van-niel@inserm.fr](mailto:guillaume.van-niel@inserm.fr)

## Summary Statement

In pigment cells, generation of PI(3,5)P2 by the PIKfyve complex regulates endosomal actin branching and associated membrane remodeling of early melanosomes. This process controls import-export balance that is required for functional amyloid formation and melanosome identity.

## Abstract

The metabolism of PI(3,5)P2 is regulated by the PIKfyve, VAC14 and FIG4 complex, whose mutations are associated with hypopigmentation in mice. These pigmentation defects indicate a key but yet unexplored physiological relevance of this complex in the biogenesis of melanosomes. Here we show that PIKfyve activity regulates formation of amyloid matrix composed of PMEL protein within early endosomes, called stage I melanosomes. PIKfyve activity controls the membrane remodeling of stage I melanosomes that increases PMEL abundance and impairs its sorting and processing. PIKfyve activity also affects stage I melanosome kiss-and-run interactions with lysosomes that is required for PMEL amyloidogenesis and establishment of melanosome identity. Mechanistically, PIKfyve activity promotes the formation and membrane tubules from stage I melanosomes and their release by modulating endosomal actin branching. Together our data indicate that PIKfyve activity is a key regulator of the melanosomal import-export machinery that fine tunes the formation of functional amyloid fibrils in melanosomes and the maintenance of melanosome identity.

Key words: PIKfyve, FIG4, VAC14, PI(3,5)P2, phosphoinositides, melanosomes, lysosomes, PMEL, amyloid, interorganelle interactions, lysosome-related organelle, endosome homeostasis, membrane deformation, endosomal tubulation, branched actin.

## Introduction

The protein complex composed of the kinase PIKfyve (Fab1), the phosphatase FIG4 (Sac3) and the scaffolding protein VAC14 (ArPIKfyve) regulates levels of phosphatidylinositol 3,5-bisphosphate (PI(3,5)P<sub>2</sub>) (Ikonomov et al., 2009; Jin et al., 2008) and PI(5)P in mammalian cells (Sbrissa et al., 2012; Zhang et al., 2007). These low abundant signaling lipids of endosomal membranes are key regulators in the homeostasis of the endolysosomal system (McCartney et al., 2014; Viaud et al., 2014). Although FIG4 acts as a PI(3,5)P<sub>2</sub> 5-phosphatase (Duex et al., 2006a; Rudge et al., 2004), its activity is also required, together with VAC14, for activation of PIKfyve (Bonangelino et al., 2002; Dove et al., 2002; Duex et al., 2006b; Jin et al., 2008). Thus, depletion not only of VAC14 and PIKfyve, but also of FIG4 reduces cellular PI(3,5)P<sub>2</sub> levels (Chow et al., 2007; Zhang et al., 2007; Zolov et al., 2012). Inhibition or depletion of the PIKfyve/VAC14/FIG4 complex (hereafter called PIKfyve complex) impairs endolysosomal functions such as endosome-to-TGN transport, endosomal homeostasis and autophagy (Ferguson et al., 2009; McCartney et al., 2014). However, the molecular mechanisms by which the PIKfyve complex controls these processes and their physiological relevance remain to be fully understood. Mouse models with mutations in VAC14 or FIG4 exhibit diluted pigmentation (Chow et al., 2007; Jin et al., 2008; Zhang et al., 2007). This hypopigmentation suggests that in melanocytes the PIKfyve complex may be involved in the biogenesis of melanosomes, in which the pigment melanin is synthesized. Our current understanding of the stepwise process of melanosome biogenesis from endosomes provides a unique opportunity to investigate the molecular origin of hypopigmentation and the role of the PIKfyve complex in the endosomal system (Bissig et al., 2016; Sitaram and Marks, 2012).

Melanogenesis involves two sequential but independent processes, functional amyloid fibril formation and pigment synthesis. Melanosomes are lysosome-related organelles that derive from early endosomes, which are called stage I melanosomes in pigment cells. During melanosome biogenesis, stage I melanosomes mature into stage II melanosomes which have acquired specific identity and morphology distinct from lysosomal organelles. Stage I melanosomes have been proposed to be the crossroad where melanosomal and endolysosomal pathways segregate (Raposo et al., 2001). However, the underlying molecular mechanisms of this segregation are

not fully understood. Stage I melanosomes are characterized by a clathrin coat and few intraluminal vesicles (ILVs) (Raposo et al., 2001). In their lumen amyloid fibril generation is initiated from cleavage products of PMEL, a transmembrane protein expressed in melanocytes (Bissig et al., 2016). During maturation into stage II melanosomes, the formation of these fibrils requires concomitant proteolytic processing of PMEL and differential sorting of PMEL cleavage products (Hurbain et al., 2008; Rochin et al., 2013; Theos et al., 2006b; van Niel et al., 2015; van Niel et al., 2011). PMEL amyloidogenesis is completed in ellipsoidal shaped stage II melanosomes where the assembled amyloid luminal fibrils serve as a matrix for pigment deposition in later stage III and IV melanosomes, which have acquired melanogenic enzymes (Raposo et al., 2001). This matrix is proposed to sequester highly reactive oxidative intermediates of melanin production, which otherwise may oxidize melanosomal content and damage organelle integrity (Fowler et al., 2006; Lee et al., 1996).

Here, we show that PIKfyve activity promotes the formation of membrane tubules emerging from stage I melanosomes and regulates their release by controlling branched actin dynamics. Interference with PIKfyve activity abrogates membrane tubule formation and branched actin-dependent release, which strongly affects stage I melanosomes homeostasis and leads to accumulation of unstructured aggregates of amyloidogenic PMEL fragments preventing amyloid matrix formation. These defects are accompanied by prolonged kiss-and-run interactions of stage I melanosomes with lysosomal compartments that affect melanosome identity and maturation.

## Results

### PIKfyve complex is required for PMEL fibril formation

To gain insight into the pigmentation defect caused by loss of VAC14 and FIG4 we used conventional electron microscopy (EM) for morphological analysis of melanosomes in the retinal pigment epithelium (RPE) in eyes of newborn mutant mice (Chow et al., 2007; Zhang et al., 2007). These melanosomes are fully mature and less susceptible to compensatory effects, as they are formed during a brief developmental period (Lopes et al., 2007). Compared to wild type (WT) RPE, we found fewer but enlarged melanosomes per  $\mu\text{m}^2$  in the RPE of *Fig4*<sup>-/-</sup> and *Vac14*<sup>-/-</sup> mice (Figure 1A-D). Enlargement of melanosomes associated with hypopigmentation is reminiscent of those observed in ocular albinism type 1 (OA1)-deficient mice (Incerti et al., 2000), where the melanin-synthesizing enzyme tyrosinase-related protein 1 (TYRP1) is mistrafficked and LAMP-1, a lysosomal protein usually poorly present in early and late melanosomes (Raposo et al., 2001) (Figure S1 left panels), is enriched in these compartments. The melanosomes in the RPE of *Fig4*<sup>-/-</sup> and *Vac14*<sup>-/-</sup> mice were also rounder than in the elongated wildtype melanosomes (Figure 1E). As reported previously for melanosomes in the RPE of mouse mutants *Bace2*<sup>-/-</sup> (Rochin et al., 2013), *PMEL silver* (Dunn, 1930) and *Pmel*<sup>-/-</sup> (Hellstrom et al., 2011), round melanosomes are indicative of a defect in PMEL fibril assembly, since the fibrils give melanosomes their characteristic ellipsoidal shape (Hellstrom et al., 2011; Theos et al., 2006a). *Vac14*<sup>L156R/L156R</sup> and *Fig4*<sup>-/-</sup> mice also exhibit the diluted coat color characteristic of certain cases of impaired PMEL fibril assembly (Chow et al., 2007; Dunn, 1930; Hellstrom et al., 2011; Jin et al., 2008; Rochin et al., 2013; Zhang et al., 2007).

To confirm these findings, we used human melanocytic cell line MNT-1 to knock down PIKfyve, VAC14 or FIG4 by RNAi (Figure 1F). In these knocked down cells (Figure 1G-H) and in MNT-1 cells treated with the PIKfyve inhibitor YM201636 (Figure S1A-E), we found more lysosomal LAMP1 and PSEN2 localized to stage II melanosomes containing processed PMEL. We also observed mislocalization of LAMP1 with the melanin-synthesizing protein TYRP1 present on pigmented melanosomes upon YM201636 treatment (Figure S1A-C). But the TYRP1 was correctly localized to pigmented melanosomes (Figure 1I) and the melanin content was unchanged (Figure 1J), excluding abnormal targeting of melanizing enzymes as in OA1 depleted MNT-1 cells (Giordano et al., 2009). As reported in MNT-1 cells

displaying a defect in PMEL fibril assembly (Rochin et al., 2013; van Niel et al., 2011), immuno-labeling with an antibody recognizing PMEL fibrils (anti-HMB45) was decreased in cells treated with RNAi against the PIKfyve complex protein when compared to control cells (Figure 1K-L). These findings indicate that the PIKfyve complex is involved in processes regulating PMEL fibril formation during early melanogenesis, which impact melanosome identity and maturation, but not pigment synthesis occurring at later steps of melanosome maturation.

### **Luminal PMEL fragments accumulate upon interference with PIKfyve function**

Generation of PMEL fibrils requires stepwise processing of PMEL by a series of proteases (Figure 2A). First, mature P2 form of PMEL is cleaved by proprotein convertase (PC) generating luminal M-alpha and transmembrane M-beta fragment that remain linked by a disulfide bond (Berson et al., 2003; Leonhardt et al., 2011; Theos et al., 2006b). Then, M-beta fragment is processed by beta-site APP-cleaving enzyme 2 (BACE2) generating a membrane-associated C-terminal fragment (CTF) and releasing amyloidogenic M-alpha into the melanosome lumen (Rochin et al., 2013). Unknown lysosomal proteases then further proteolytically process M-alpha into amyloidogenic peptides that finally assemble into fibrils (Ho et al., 2016; Kawaguchi et al., 2015; Leonhardt et al., 2013). Given the reported involvement of PIKfyve complex in endolysosome homeostasis (Bissig et al., 2017; Jefferies et al., 2008), we studied whether PIKfyve inhibition or knockdown would affect PMEL processing.

Using a set of antibodies that recognize distinct epitopes and processed fragments of PMEL (Figure 2B) we found that PIKfyve complex knockdown or inhibition for 2 h and 24 h did not affect PC- and BACE2-mediated PMEL cleavage producing M-alpha, M-beta and CTF fragments, but caused an accumulation of the CTF (Figure 2C and S1G) that is not part of PMEL fibrils and of M-alpha (Figure S1G). Due to their amyloidogenic nature, PMEL fibril associated fragments distribute to the Triton X-100 insoluble fraction in cell lysates (Berson et al., 2003; Leonhardt et al., 2013; Watt et al., 2009). In this fraction, we found accumulation of M-alpha, M-alphaN, M-alphaC (Figure 2D and S1H). Treatment of MNT-1 cells for 2 h and 24 h with a mix of lysosomal protease inhibitors (100  $\mu$ M leupeptin, 10  $\mu$ M pepstatin A and 10  $\mu$ M E-64d) led to a similar accumulation CTF, M-alpha, M-alphaN and M-alphaC (Figure 2E-F) but decreased generation of RPT and PKD fragments. These results confirm

that lysosomal proteases are required for PMEL processing (Ho et al., 2016; Kawaguchi et al., 2015; Leonhardt et al., 2013), and suggest that accumulation of processed and non-processed fragments of PMEL luminal domain under PIKfyve inhibition may be caused by changes of lysosomal activity.

### **Lysosomal activity is not affected upon inhibition of PIKfyve**

We assessed the lysosomal functions of melanocytes treated with YM201636. In these cells neither the number nor the size of LAMP1 compartments significantly changed upon inhibition of PIKfyve activity (Figure 3A-D). Using ratiometric fluorescence imaging we detected similar pH of endolysosomes in mock and YM201636 treated cells ( $4.4 \pm 0.2$  and  $4.5 \pm 0.2$ , respectively) (Figure S2A-B) in good agreement with previous reports (Bissig et al., 2017; Ho et al., 2015). Internalization of proteolytically dequenched DQ-BSA showed that treatment with PIKfyve inhibitor slightly increased proteolysis of endocytosed DQ-BSA, although the effect was not statistically significant (Figure S2C-D). The levels of mature cathepsin D (CatD) decreased and immature CatD accumulated upon treatment with lysosomal protease inhibitors, but not upon YM201636 treatment (Figure S2E), indicating that PIKfyve inhibition does not impair endolysosomal activity. To reinforce these results, we assessed steady-state levels of the melanocyte specific transmembrane protein MART1, which is ubiquitylated and degraded in lysosomes (Levy et al., 2005). PIKfyve inhibition, in contrast to inhibition of lysosomal proteases did not cause MART1 accumulation (Figure S2E). The trafficking of fluid phase marker (DextranAF647) (Figure S2F-G) or lysosomal transmembrane protein (PSEN2) (Figure S2H-I) to lysosomes was not affected upon YM201636 treatment, showing that PIKfyve inhibition neither affected transport of endocytosed cargo to endolysosomes nor trafficking of lysosomal resident proteins. This set of data shows that inhibition of PIKfyve does not impair lysosomal activity, excluding lysosomal dysfunction as a cause for accumulation of PMEL fragments.

### **Lysosomal activity is delivered to melanosomes through kiss-and-run**

Others and our data show that lysosomal protease activity is required for PMEL processing and fibril formation in stage I melanosomes (Ho et al., 2016; Leonhardt et al., 2013). However, in melanocytes lysosomes and melanosomes co-exist as separate entities with distinct content and morphology (Raposo et al., 2001). In line

with this, immuno-labeling of M-alpha species revealed their accumulation in EEA1, but not LAMP1 labelled compartments at steady state and upon inhibition of PIKfyve activity (Figure 3A-B, E-F). We speculated that PMEL localized in stage I melanosomes may be processed by lysosomal proteases through transient interactions of stage I melanosomes and endolysosomes, which could be affected by YM201636 treatment.

We tested this hypothesis by live-cell imaging of MNT-1 cells co-expressing LAMP1-mRuby2 and the PI(3)P-binding protein 2xFYVE-GFP, as markers for endolysosomes and stage I melanosomes, respectively. We confirmed in fixed cells that 2xFYVE-GFP is found on stage I melanosomes, which correspond to early endosomes in pigment cells and contain mature PMEL and M-alpha (Figure S3A-B). In contrast, 2xFYVE-GFP did not co-localize with endolysosomes or with later stages melanosomes containing fully formed PMEL fibrils or melanin synthesizing enzymes or endolysosomes (Figure S3C-F). Our live-cell imaging revealed that in mock treated cells 2xFYVE-GFP and LAMP1-mRuby2 compartments transiently interact for on average 4.0 sec without undergoing complete compartment mixing (Figure 3I,K and movie 1-2). To assess whether membrane fusion occurs, endolysosomes of 2xFYVE-GFP expressing cells were loaded by pulse-chase with DextranAF555 and transfer of endolysosomal DextranAF555 to 2xFYVE-GFP compartments was monitored by live-cell microscopy. We found that endolysosomal DextranAF555 can be transferred to 2xFYVE-GFP compartments (Figure 3L-M and movie 3), showing that membrane fusion between the two compartments occurs. These findings support our hypothesis that the substrate PMEL, localized to stage I melanosomes is processed by lysosomal proteases through transient fusions of stage I melanosomes and endolysosomes. These interorganellar kiss-and-runs strengthen the role of stage I melanosomes as crossroad between melanosomal and endolysosomal pathways and provides mechanistic insights into the segregation of both pathways.

In YM201636 treated cells, stage I melanosomes and endolysosomes transiently interacted. However, the time of contact doubled when compared to mock (10.0 sec vs 4.0 sec), but was restored upon YM201636 washout and re-synthesis of PI(3,5)P2/PI(5)P (Figure 3J-K and S3G and movies 4-7). Moreover, upon PIKfyve inhibition the two compartments still transiently fused, as illustrated by the transfer of endolysosomal DextranAF555 (Fig 3N-O and movie 8).

These data show that accumulation of processed and unprocessed PMEL/M-alpha

species in stage I melanosomes upon PIKfyve inhibition did not result from impaired transient fusion between stage I melanosomes and endolysosomes. However, the prolonged duration of contact between stage I melanosomes and endolysosomes upon inhibition of PIKfyve activity may cause over time the observed mislocalization of endolysosomal proteins to melanosomes and loss of melanosome identity.

### **PMEL fragments accumulate in enlarged EEA1 compartments**

The absence of defect of lysosomal activity and morphology upon inhibition of PIKfyve activity led us investigate potential defect of the EEA1 compartments where PMEL fragments accumulated upon treatment. Interestingly, immuno-labeling showed that EEA1-positive compartments that accumulated PMEL/M-alpha species following YM201636 treatment (Figure 3E-F) were enlarged and less numerous when compared to control (Figure 3G-H). In good agreement with this, after PIKfyve inhibition by YM201636 treatment we observed enlargement of 2xFYVE-GFP-positive stage I melanosomes, but not LAMP1-mRuby2-positive endolysosomes in our live-cell imaging experiments (Figure 3J).

It is thus conceivable that PIKfyve activity directly regulates stage I melanosome homeostasis explaining the lack of PMEL fibrillation when PIKfyve function is impaired.

To better characterize the apparent defect in early melanosomes, we performed EM analysis of resin embedded and chemically fixed MNT-1 cells knocked down for PIKfyve, VAC14 or FIG4 by RNAi or treated with the PIKfyve inhibitor YM201636 (Figure 4A-B). In MNT-1 cells, melanosome biogenesis occurs continuously. Therefore, all four melanosome maturation stages are present and can morphologically be distinguished by EM. We observed enlarged ILV containing stage I melanosomes decorated with a clathrin coat in inhibitor or RNAi treated cells (Figure 4A-B). Of note the mean size increase was only significant for YM201636 treatment and PIKfyve knockdown (Figure 4C). Similarly, stage I melanosomes were enlarged in human primary melanocytes knocked down for VAC14, FIG4 and PIKfyve (Figure 4F). In addition, MNT-1 cells treated with RNAi for the PIKfyve complex proteins displayed fewer fibril-containing stage II melanosomes, but more unpigmented melanosomes with unstructured luminal aggregates (Figure 4D-E), further confirming our findings that the PIKfyve complex is involved in PMEL fibril formation (Figure 1K-L). In line with our observations that the PIKfyve complex is not

involved in pigment synthesis (Figure 1I-J), interference with PIKfyve complex did not alter the number and morphology of pigmented melanosomes (Figure 4A-B and E). These morphological observations show that the PIKfyve complex is required for stage I melanosome homeostasis and PMEL fibril formation, which is initiated in these compartments.

PMEL fibrillation results from concomitant processing and sorting of the amyloidogenic luminal domain of PMEL to ILVs of stage I melanosomes (Hurbain et al., 2008; Rochin et al., 2013; Theos et al., 2006b; van Niel et al., 2015; van Niel et al., 2011). Ultrathin cryosections of MNT-1 cells confirmed the presence of ILV in stage I melanosomes labeled by anti-PMEL-N antibody (Figure 4G-H), indicating that PIKfyve activity is not critical for ILV formation. These data also revealed that upon PIKfyve inhibition mature PMEL/M-alpha is localized to enlarged clathrin-coat containing stage I melanosomes, where it was mostly found on the limiting membrane and to a lesser extent on ILVs (Figure 4G-H). However, a similar amount of gold labeling was found on ILVs between YM201636 treated and control condition (Figure 4I), suggesting that PMEL/M-alpha sorting to ILVs is not impaired. However, accumulation of this fragment on the limiting membrane may indicate a saturation of the sorting machinery.

Altogether, our results suggest that upon interference with the PIKfyve complex luminal PMEL fragments accumulate in enlarged stage I melanosomes causing unstructured PMEL aggregation preventing fibril formation and impairing melanosome maturation.

### **PIKfyve activity promotes membrane remodeling**

Our observations show that upon PIKfyve inhibition the size of stage I melanosomes doubles, their number decreases and they accumulate PMEL fragments. A similar organelle enlargement induced by inhibition of PIKfyve activity was observed for endolysosomes in HeLa cells. In these cells PIKfyve activity was shown to control endolysosome homeostasis by promoting membrane remodeling (Bissig et al., 2017). Thus, we hypothesized that PIKfyve exerts a similar function on stage I melanosomes and we studied stage I melanosome homeostasis and membrane dynamics by live-cell microscopy using 2xFYVE-GFP. In mock treated cells these compartments were highly dynamic and underwent frequent homotypic fusion and fission (Movie 9). Their shape was heterogeneous, and they were often tubulated

(Figure 5A-B). These features were lost upon inhibition of PIKfyve activity, where stage I melanosomes were fewer, enlarged, spherical and lacked membrane tubules (Figure 5A-D). In addition, the compartments were less dynamic as compared to control (Movie 10). Upon YM201636 washout and re-synthesis of PI(3,5)P<sub>2</sub>/PI(5)P membrane dynamics was restored and tubules and buds were formed and released resulting in recovery of compartment size and number (Figure 5A-D and movie 11). These findings indicate that PIKfyve activity promotes membrane remodeling of stage I melanosomes required to maintain compartment size, number and homeostasis during homotypic fusion-fission processes of stage I melanosomes. To confirm these findings, we performed electron microscopy analyses on high-pressure frozen and freeze-substituted melanocytes, because this technique optimally preserves subtle membrane deformation such as membrane tubulations. In mock treated cells multivesicular stage I melanosomes often displayed tubules and bore a clathrin coat on their limiting membrane. In contrast after YM201636 treatment these compartments lost their tubular appearance and were enlarged, but still displayed clathrin coats. Upon YM201636 washout the tubular feature was restored and dividing enlarged compartments were observed (Figure 5E-H), showing that PIKfyve activity is required for membrane remodeling on stage I melanosomes. We assessed the contribution of this membrane remodeling to PMEL accumulation by performing immunofluorescence microscopy. YM201636 induced accumulation of PMEL fragments in these enlarged EEA1-positive stage I melanosomes that were both rescued after drug washout and PI(3,5)P<sub>2</sub>/PI(5)P re-synthesis (Figure 5I-K). These findings confirm that PIKfyve activity controls stage I melanosome size, number and dynamics by regulating fission processes of stage I melanosomes. Interference with PIKfyve activity by inhibiting the homotypic fission induce the accumulation of PMEL fragments in fewer but larger stage I melanosomes that would contribute to the impaired PMEL fibrillation.

### **PIKfyve activity controls endosomal branched actin required for tubule release**

To refine the mechanisms involved in the inhibition of PMEL fibrillation upon PIKfyve activity we explored the downstream and upstream pathways regulated by this complex such as the activation of mucolipin channels by PI(3,5)P<sub>2</sub> (Dong et al., 2010), PI(3)P levels (Zolov et al., 2012), pH (Jefferies et al., 2008) or endosomal actin branching (Hong et al., 2015). In MNT-1 cells, co-treatment of YM201636 with

the mucolipin activator MLSA1 did not restore stage I melanosome size and membrane dynamics (Figure S4A-B). These findings indicate that mucolipins may not be downstream effectors of PIKfyve activity in melanosome biogenesis, which is in line with our observations in HeLa cells (Bissig et al., 2017). Ratiometric fluorescence imaging with a short pulse-chase protocol excluded a pH defect in stage I melanosomes as a cause of impaired fibrillation of PMEL (Figure S4C). Inhibition of PIKfyve activity was shown to cause a slight increase in the PI(3,5)P<sub>2</sub> substrate PI(3)P in some, but not all cell types (Jefferies et al., 2008; Zolov et al., 2012). Upon inhibition of PIKfyve activity we did not observe any change in the localization or intensity of fluorescence associated to endogenous protein EEA1 nor to 2xFYVE-GFP that both bind PI3P (Figure S4D). Similarly, biochemical analysis showed no significant differences in membrane recruitment of endogenous EEA1 and expressed 2xFYVE-GFP between DMSO and YM201636 treated cells (Figure S4E-F). These results show that localization of PI(3)P-binding proteins is unaffected upon PIKfyve inhibition and indicate that in melanocytes PI(3)P does likely not accumulate upon PIKfyve activity inhibition.

Recently, PI(3,5)P<sub>2</sub> has been shown to control dynamics of branched actin on endosomal membranes (Hong et al., 2015), which is itself involved in various membrane remodeling processes (Anitei and Hoflack, 2011). Thus, we asked whether PIKfyve activity promotes membrane remodeling through regulation of endosomal actin dynamics. As observed in human breast adenocarcinoma cells (Hong et al., 2015), we found that actin patches accumulated on EEA1-positive and enlarged stage I melanosomes upon PIKfyve inhibitor treatment. Actin accumulation was abolished upon inhibition of the Arp2/3 complex by treatment with CK666 (Figure 6A). These data reveal that in melanocytes as in other cells PI(3,5)P<sub>2</sub>/PI(5)P regulates branched endosomal actin.

We performed live-cell imaging of 2xFYVE-GFP transfected cells to study whether endosomal actin is involved in PI(3,5)P<sub>2</sub>/PI(5)P-mediated membrane remodeling. Stage I melanosomes of cells treated with the Arp2/3 inhibitor CK666 still displayed membrane tubules. Similarly, when YM201636 was washed out in the presence of CK666, membrane tubules were observed (Figure 6B and 6C-E), showing that endosomal branched actin is not required for PI(3,5)P<sub>2</sub>/PI(5)P-mediated membrane remodeling. However, upon inhibition of branched actin dynamics by CK666 treatment, membrane buds and tubules were less readily released and often

collapsed (Figure 6C-E and movie 12-15), suggesting that endosomal actin dynamics is involved in membrane tubule release.

Electron microscopy analyses of high-pressure frozen MNT-1 cells confirmed that upon inhibition of Arp2/3 complex tubules are formed on stage I melanosomes (Figure 6F). Similarly, membrane tubules on enlarged stage I melanosomes were observed upon YM201636 washout in the presence of CK666 (Figure 6F), but stage I melanosomes were still enlarged after 4 h YM201636 washout in the presence of CK666, indicating that although membrane tubules are formed the compartment size was not rescued (Figure 6F), probably because the tubules were less readily released. Immunofluorescence microscopy showed that YM201636 induced accumulation of PMEL in EEA1-positive stage I melanosomes and their enlargement were rescued after drug washout and PI(3,5)P2/PI(5)P re-synthesis. However, both accumulation of PMEL and enlargement of EEA1-positive stage I melanosomes persisted when YM201636 was washed out in the presence of Arp2/3 complex inhibitor (Figure 6G-I), showing that PI(3,5)P2/PI(5)P-mediated membrane remodeling and endosomal actin dynamics are involved in the same pathway. Thus, our findings indicate that PI(3,5)P2/PI(5)P spatially and temporally coordinates membrane remodeling and actin-dependent release of endosomal tubules and buds, which is required for stage I melanosome homeostasis and PMEL fibril formation.

## **Discussion**

Our data show that the formation of PMEL amyloid fibrils and melanosome identity rely on tight regulation of the homeostasis of stage I melanosomes and their transient interaction with lysosomes. By controlling membrane remodeling at stage I melanosomes, PIKfyve activity balances the import of lysosomal proteases and the steady state level of their substrate, PMEL, and thereby regulates the formation of amyloid matrix and the preservation of melanosome identity (Figure 7). Functionally, PIKfyve activity regulates morphology, size and number of stage I melanosomes by promoting the formation of membrane tubules and buds that are released in a mechanism involving branched endosomal actin dynamics (Figure 7 inset). Inhibition of PIKfyve activity abrogates membrane remodeling, causing an imbalance favouring stage I melanosomes homotypic fusion over fission that reduces the number and increases the size of stage I melanosomes. The imbalance between homotypic fusion and fission causes accumulation of PMEL that saturates amyloidogenic processing and sorting machineries. These defects result in accumulation and aberrant aggregation of amyloidogenic PMEL fragments impairing fibril formation.

### **Interorganelle interactions ensure PMEL amyloid formation**

The data presented here confirm the requirement of lysosomal proteases for PMEL processing and amyloid formation, although their localization is separated from PMEL (Ho et al., 2016; Kawaguchi et al., 2015; Leonhardt et al., 2013; Raposo et al., 2001). We describe a model in which transient kiss-and-run interactions and fusions between endolysosomes and PMEL-containing stage I melanosomes ensure PMEL processing by lysosomal proteases. These transient interactions provide a dynamic means to coordinate melanosome maturation with PMEL processing and fibril formation and thus ensure proper amyloid assembly. The kiss-and-run interactions that we describe do not lead to full fusion of both compartments and are thus consistent with previous observations that endolysosomes and melanosomes co-exist as distinct, but proximate organelles in melanocytes (Raposo et al., 2001). By regulating interorganelles interaction, the PIKfyve activity appears as a key element of the acquisition of melanosome identity.

Inhibition of PIKfyve activity results in longer interorganelle contacts, which correlates with mislocalization of endolysosomal proteins to melanosomes. Such impaired segregation of melanosomal and lysosomal cargo was suggested to affect

PMEL fibril formation and early melanogenesis (Giordano et al., 2009). One can imagine that the increased lysosomal character of maturing melanosomes may affect PMEL assembly rates.

### **PIKfyve activity promotes membrane remodeling**

Our data demonstrate that PIKfyve activity promotes membrane remodeling and tubule formation required to maintain stage I melanosome number, homeostasis and function in melanocytes. The molecular mechanism by which PIKfyve activity induces the formation of membrane tubules in mammalian cells still remains elusive. PI(3,5)P<sub>2</sub> produced by PIKfyve activates transient receptor potential mucolipin (TRPML) channel family and mice carrying a mutation in TRPML3, which is highly expressed in melanocytes, show pigmentation abnormalities (Di Palma et al., 2002; Dong et al., 2010). Activation of the TRPML protein family by the small molecule activator MLSA1 was shown to rescue the enlarged compartment phenotype of PI(3,5)P<sub>2</sub>-depleted FIG4 and VAC14 knockout cells (Dong et al., 2010; Zou et al., 2015). However, in melanocytes MLSA1 co-treatment with YM201636 neither counteracted stage I melanosome enlargement nor rescued membrane tubule formation (Figure S4A-B). These findings indicate that during melanosome biogenesis, TRPMLs may not be downstream effectors of PIKfyve activity, which is in line with our observations in HeLa cells (Bissig et al., 2017). It is worth noting that mice mutant for TRPML3, VAC14 and FIG4 exhibit different fur pigmentation phenotypes (Atiba-Davies and Noben-Trauth, 2007; Chow et al., 2007; Jin et al., 2008; Zhang et al., 2007), which may reflect distinct molecular roles. PI(3,5)P<sub>2</sub> was also shown to activate melanosomal two-pore sodium channel 2 (TPC2) that negatively regulates pigmentation (Bellono et al., 2016). However, TPC2 acts mainly on pigmented melanosomes, whereas PIKfyve activity is involved in homeostasis of unpigmented melanosomes and inhibition of PIKfyve activity does not impair melanin production.

It is attractive to speculate that PI(3,5)P<sub>2</sub> synthesis by PIKfyve triggers the recruitment of PI(3,5)P<sub>2</sub>-binding effector proteins, which may have membrane bending properties, as shown for the BAR domain of SNX1 involved in retrograde transport (Carlton et al., 2004). Recently, the PROPPIN domain of yeast Atg18, which binds PI(3)P and PI(3,5)P<sub>2</sub>, was shown to drive membrane tubule formation and fission via bilayer insertion of an amphipathic alpha-helix and oligomerization

(Gopaldass et al., 2017). This membrane deformation and fission function may be shared by other PROPPINs, such as the mammalian WIPI proteins, which also contain potential amphipathic alpha-helical features. Interestingly, mammalian WIPI1 is involved in early melanogenesis and is thus a promising PI(3,5)P2 effector in melanocytes (Ho et al., 2011).

Our data further provide evidence that membrane tubules generated by PIKfyve activity are released by a mechanism involving branched actin dynamics. As PI(3,5)P2 regulates endosomal branched actin, it is likely that PIKfyve activity also controls actin-dependent membrane release. A role of actin in membrane release is exemplified by the fission of Shiga-toxin carriers induced by actin-driven lipid phase separation (Allain et al., 2004; Romer et al., 2010; Roux et al., 2005) and in endosomal fission associated to ER contact sites (Rowland et al., 2014). The actin network may also promote membrane reorganization and neck constriction by inducing mechanical forces, which may involve the action of actin-based motors (Derivery et al., 2009; Ripoll et al., 2018). In that respect it is interesting to note that overexpression of myosin 1b affects early endosome morphology, slows PMEL processing and impairs PMEL fibril formation (Salas-Cortes et al., 2005) – phenotypes reminiscent of PIKfyve inhibition.

### **PIKfyve mediated membrane remodeling is required for formation of PMEL amyloid matrix**

Our study provides evidence that formation of early melanosomal membrane tubules initiated by PIKfyve activity is co-ordinated with PMEL amyloid assembly and melanosome maturation. Similarly, endosome maturation was described to be co-ordinated with endosome tubule formation (van Weering et al., 2012), indicating that melanocytes have fine-tuned a ubiquitous endosomal process for melanosome biogenesis. Membrane tubules formed during endosome maturation serve cargo sorting to different cellular locations, which is ensured by the assembly of various sorting machineries. In melanocytes, tubules emerging in an actin dependent manner from recycling endosomes transport melanogenic enzymes, transporters and accessory proteins to melanosomes for pigment synthesis (Delevoye et al., 2016; Dennis et al., 2016; Setty et al., 2007; Sitaram et al., 2012). These tubules are, however, distinct from the PIKfyve-driven tubules described here, as we do not observe any defect in pigment synthesis. Endosomal tubules formed by PIKfyve

activity are involved in endosome-to-TGN retrograde transport (de Lartigue et al., 2009; Rutherford et al., 2006), a process that also involves endosomal actin network (Seaman et al., 2013). However, such retrograde transport has not been described for PMEL. The membrane remodeling initiated by the PIKfyve activity contributes here to homotypic fusion-fission processes that allow a homogenous repartition of PMEL within the small and highly dynamic population of stage I melanosomes. Impaired membrane remodeling results then in the accumulation of PMEL luminal fragments in enlarged, immotile and fewer stage I melanosomes. This accumulation saturates PMEL processing and sorting machinery and leads to aberrant aggregation of PMEL and thus a defect in PMEL fibril formation and melanosome maturation. Interestingly, evidence suggests that terminal proteolytic maturation of luminal PMEL fragments only occurs after aggregation into a pre-matrix (Leonhardt et al., 2013). Thus, impaired pre-matrix assembly may lead to accumulation of partially processed luminal PMEL fragments that aberrantly aggregate due their amyloidogenic nature.

### **Implications for pathological amyloid formation**

The PMEL fibrils that assemble within melanosomes are amyloids (Fowler et al., 2006). In contrast to pathological amyloids that are associated with neurodegenerative diseases such as Alzheimer's, Parkinson's or Huntington's disease, PMEL amyloid fibrils are not pathogenic and serve beneficial functions. They are thus called functional or physiological amyloids. Nevertheless, the amyloidogenic nature of PMEL presents a potential danger for the cell, as aberrant aggregation may be toxic (Watt et al., 2011). It is possible that long-term inhibition of PIKfyve activity may damage melanosome integrity by accumulation of toxic PMEL aggregates and/or melanin intermediates, perhaps leading to melanocyte death. Interestingly, mice uniquely knockout for PIKfyve in pigment cells (Liggins et al., 2018) exhibit hair greying that is similar to mouse models with impaired PMEL fibril (Rochin et al., 2013) and their melanocytes display vacuolar compartments that are reminiscent of our observations. Lower melanocyte survival rates may also explain why VAC14 and FIG4 mutant mice show hypopigmentation phenotypes, while we did not observe impaired pigment synthesis. Since PMEL fibrils sequester melanin and thus might facilitate melanin transfer to keratinocytes, fur hypopigmentation may also result from inefficient pigment transfer. These two models are not mutually

exclusive.

In view of the interesting similarities between intracellular trafficking and processing of PMEL and amyloid precursor protein (APP), which is involved in Alzheimer's disease (Bissig et al., 2016; Sannerud et al., 2016), our studies may also have important implications for pathological amyloid formation during Alzheimer's disease. Intriguingly, PIKfyve depletion leads to massive neurodegeneration in individuals with mutations of FIG4 and VAC14 (Baulac et al., 2014; Campeau et al., 2013; Chow et al., 2007; Lenk et al., 2011; Lenk et al., 2016) and PIKfyve influences APP (Balklava et al., 2015; Currinn et al., 2016). It is therefore tempting to speculate that, in neurons, PIKfyve activity regulates the abundance of an amyloidogenic substrate and its proteases in a compartment known to generate the Abeta intracellular pool (Peric and Annaert, 2015; Rajendran and Annaert, 2012; Sannerud et al., 2016). Further work will determine whether PIKfyve activity plays analogous roles in physiological and pathological amyloid formation.

## **Materials and Methods**

### **Cell culture, transfections and drug treatment**

Human melanocytic MNT-1 cells and primary melanocytes were maintained as previously described (Berson et al., 2001; Raposo et al., 2001; van Niel et al., 2015). Cells were transfected according to manufacturer's recommendation with DNA and siRNA using JetPrime (Polyplus transfection TM) and oligofectamine (Invitrogen), respectively. Experiments were performed 16h after transfection with DNA. siRNA transfections were performed twice at 48h interval and experiments were performed 96h after the first siRNA transfection. If not otherwise indicated, cells were incubated for 2h with 1.6  $\mu$ M YM201636 (Abcam), 200  $\mu$ M CK-666 (Tocris), 1 $\mu$ M Vps34 inhibitor (IN1, Calbiochem) or DMSO (Sigma-Aldrich). YM201636 was washed out for 1h to 4h at 37°C after 3 washes with cold medium. If indicated 200  $\mu$ M CK-666 (Tocris) was present during the washout.

### **Reagents, antibodies, siRNAs and plasmids**

Reagents were obtained from the following sources: DAPI (4',6-diamidino-2-phenylindole), Dextran 10'000 MW conjugated to Alexa Fluor 488, 555 or 647 and DQ-BSA from Thermo Fisher Scientific; YM201636 from Abcam; MagicRed probe from Immuno Chemistry Technologies; CK-666 from Tocris; IN1 from Calbiochem; pepstatinA and E-64d from Calbiochem; leupeptin from Euromedex and other reagents were obtained from Sigma-Aldrich.

Antibodies were obtained from the following sources: anti-FIG4 (ab186269), anti-VAC14 (ab67369), anti-Melanoma (HMB45) (ab787), anti- $\beta$ -TUB (ab6046), anti-PSEN2 (ab51249), anti-TYRP1 (ab3312), anti-EEA1 (Ab70521) antibodies and horseradish peroxidase (HRP)-conjugated goat polyclonal antibodies to rabbit IgG (ab6721) and to mouse IgG (ab6789) from Abcam; anti- PMEL NKI from Neomarkers, anti-PIKfyve antibody (PCR-PIKFYVE-3C9) from Developmental Studies Hybridoma Bank (DSHB); mouse anti-LAMP1 antibody (555798) from BD Biosciences; secondary goat anti-rabbit or anti-mouse antibodies conjugated to Alex Fluor 488, 555 or 647 were from Thermo Fisher Scientific. Protein A conjugated to 15 nm gold particles (PAG15) and BSA conjugated to 5 nm gold particles (BSA-gold 5nm) were from Cell Microscopy Center (AZU, Utrecht University, Netherlands); Affinity-purified anti-peptide antibodies recognizing the PMEL N-terminus (anti-

PMEL-N) (Berson et al., 2003) and C-terminus (anti-PMEL-C) (Raposo et al., 2001) were described previously.

The siRNAs targeting FIG4 (L019141), VAC14 (L015729), PIKfyve (L005058) and non-targeting control (D001810) ON-TARGET plus SMARTpool were from Thermo Fisher Scientific.

The 2xFYVE-GFP (Gillooly et al., 2000) and LAMP1-mRuby2 (Lam et al., 2012) (Addgene plasmid #55902) plasmid were kind gifts from Harald Stenmark and Michael Davidson, respectively.

### **Dextran internalization assays**

Dextran internalization for Dextran transfer experiments: To internalize Dextran 10'000MW AF555 into endolysosomes, MNT-1 cells were pulsed with 1mg/ml Dextran-AF555 at 37°C for 4h, washed 3 times with cold medium and chased with conjugate-free medium for 20h at 37°C (Bright et al., 2005).

Dextran-AF647 co-internalization with DQ-BSA: MNT-1 cells were pretreated for 2h with 1.6µM YM201636 or DMSO. Then Dextran-AF647 and DQ-BSA were co-internalized at a concentration of 50µg/ml each for 2h at 37°C. Cells were washed 3 times with cold medium and incubated for 1h with conjugate-free medium at 37°C. Snapshots of live-cells were taken at 37°C in imaging buffer (20mM HEPES-NaOH pH 7.4 140mM NaCl, 2.5mM KCl, 1.8mM CaCl<sub>2</sub>, 1.0mM MgCl<sub>2</sub>, 4.5g/L D-Glucose). YM201636 or DMSO was present throughout the experiment.

### **Electron microscopy**

For conventional EM, MNT-1 were grown on coverslips, fixed in 2.5% glutaraldehyde in 0.1 M cacodylate buffer for 24 h, post-fixed with 1% osmium tetroxide, dehydrated in ethanol and embedded in epon as described (Raposo et al., 2001). For EM analysis of RPE sections, tissues from newborn mice were processed as previously (Rochin et al., 2013) For high-pressure freezing MNT-1 cells were grown on carbonated sapphire discs (30 mm in diameter) and high-pressure frozen using a HPM 100 (Leica Microsystems) or HPM Light µ (CryoCapCell) in FBS serving as filler. High-pressure frozen samples were transferred to an AFS (Leica Microsystems) with precooled (-90°C) anhydrous acetone containing 2% osmium tetroxide and 1% H<sub>2</sub>O. Freeze substitution and epon embedding was performed as described (Hurbain et al., 2008). Ultrathin sections of cell monolayers or RPE were

prepared with a Reichert UltracutS ultramicrotome (Leica Microsystems) and contrasted with uranyl acetate and lead citrate.

For ultrathin cryosectioning and immunogold labeling, cells were fixed in 2% PFA, 0.2% glutaraldehyde in 0.1M phosphate buffer pH 7.4. Cells were processed for ultracryomicrotomy and immunogold labeled using PAG 15 as described (Raposo et al., 2001).

All samples were examined with a FEI Tecnai Spirit electron microscope (Thermo Fisher Scientific), and digital acquisitions were made with a numeric camera (Quemesa; EMSIS).

### **Live cell microscopy and immunofluorescence analysis**

MNT-1 cells grown on coverslips were fixed with 2% PFA, permeabilized with 0.05% saponin/1% BSA in PBS, quenched with 50mM glycine and processed for indirect immunolabeling. Images were captured on a LSM 780 confocal microscope (Zeiss) using an oil-immersion plan Apo 63x A/1.40 NA objective lens.

Live-cell imaging experiments were done in fluorodishes (World Precision Instruments) at an inverted spinning disc microscope (Nikon) using an oil-immersion plan Apo 100x A/1.40 NA objective lens. Live-cell imaging was performed at 37°C in imaging buffer (20mM Hepes-NaOH pH 7.4 140mM NaCl, 2.5mM KCl, 1.8mM CaCl<sub>2</sub>, 1.0mM MgCl<sub>2</sub>, 4.5g/L D-Glucose) and movies were taken at 0.4s frame rate for 2min. Data were collected using Metamorph Software and analyzed using ImageJ, Icy and CellProfiler software.

### **Image analysis and quantification**

Melanosome stages were defined by morphology (Raposo et al., 2001; Seiji et al., 1963). Length and width of melanosomes, as well as the size were measured using ImageJ software. To measure contact times, organelles were segmented using Icy software and the time that two organelles partially overlap was assessed. The size of organelles was measured after segmentation using Icy software. Colocalization was quantified using CellProfiler software calculating the correlation coefficient. Dextran transfer to 2xFYVE-GFP compartments (defined as ROI) was quantified measuring the fluorescence intensity of the Dextran channel in the ROI using ImageJ. P values were determined by Student's t-test, unpaired, unequal variance (\*p<0.05, \*\*p<0.01, \*\*\*p<0.001).

## **Other methods**

### Western blot:

For Western blots a Triton X-soluble lysate was prepared in 20 mM Tris-HCl pH 7.4, 150 mM NaCl, 1% TX-100, 1 mM EDTA, protease inhibitors. The Triton X-insoluble fraction was resuspended in 1% SDS, 1% B-mercaptoethanol in PBS containing protease inhibitors, incubated for 10 min at RT and then heated for 10 min at 100°C.

### Membrane-cytosol fractionation

Cells are scraped and centrifuged at 900 rpm for 5min at 4°C. The pellet is homogenized in homogenization buffer (0.25M sucrose, 10mM Hepes-NaOH pH 7,4) and then centrifuged at 2000 rpm for 10min at 4°C. The pellet is resuspended in the homogenization buffer and after centrifugation at 2000 rpm for 10min, the Post Nuclear Supernatant (PNS) is collected and centrifuged at 53000 rpm for 1h at 4°C. The supernatant (cytosol fraction) is collected and the pellet (membrane fraction) is resuspended in (10mM Tris-HCL pH7.4, 150mM NaCl, 0.5mM EDTA) solution containing protease inhibitors.

### Melanin assay:

Cells were disrupted by sonication in 50 mM Tris-HCl, pH 7.4, 2 mM EDTA, 150 mM NaCl, 1 mM DTT, and protease inhibitors. Pigment was pelleted at 16000g for 15min at 4°C, rinsed once in ethanol/ether (1:1), and dissolved in 2M NaOH/20% DMSO at 60°C. Melanin content was measured as optical density at 492nm.

### Ratiometric pH measurement:

pH-sensitive fluorophore Oregon green 488 (DextranOG) and pH-insensitive fluorophore Alexa Fluor 647 (DextranAF647) were internalized and imaged as described above in Dextran internalization assays. To convert fluorescence values to pH the emission of the two dyes was recorded separately and the fluorescence ratio was converted to pH using an internal calibration curve. To acquire the calibration curve cells were sequentially bathed for 5min in 143mM KCl, 5mM glucose, 1mM MgCl<sub>2</sub>, 1mM CaCl<sub>2</sub>, 20mM Hepes buffered to a pH ranging from 4.0 to 7.5 and containing 10µM nigericin and 5µM monensin.

### **Author contributions**

C.B. conceived, designed, performed and analyzed data from all experiments and wrote the manuscript. P.C. designed, performed and analyzed some experiments. I.H and X.H. helped to perform HPF and related EM. R.S. performed some experiments. G.L. and E.K. provided essential mouse biopsies. W.A., M.M., L.W. and G.R. edited and reviewed the manuscript. G.v.N. conceived and supervised the project, analyzed data and wrote the manuscript.

### **Acknowledgements**

We are grateful to Michael S. Marks and Cedric Delevoye for fruitful discussions and critical reading of the manuscript. We thank the PITC-IBiSA Imaging Facility, the Institut Curie (Paris), the Nikon Imaging Center and the members of the France-Biolmaging national research infrastructure for assistance with microscopy.

### **Competing interests**

The authors declare no competing interests

### **Funding**

This work was supported by Institut Curie, CNRS, by the Fondation ARC pour la Recherche sur le Cancer (grant SL220100601359) (to GR), by the Fondation pour la Recherche Médicale (AJE20160635884) (to GvN), by a Research Grant from the Amyloidosis Foundation (to GvN), by the French National Research Agency through the "Investments for the Future" program (France-Biolmaging, ANR-10-INSB-04)", the CeITisPhyBio Labex (N° ANR-10-LBX-0038) part of the IDEX PSL (N°ANR-10-IDEX-0001-02 PSL)", the Swiss National Fund for Research for the Early Postdoc. Mobility fellowship P2GEP3-151589 and the Advanced Postdoc. Mobility fellowship P300PA\_167618 (to CB), the Federation of European Biochemical Societies for the Long-Term Fellowship (to CB) and Labex CeITisPhyBio for the post-doctoral fellowship (CB). WA and RS are supported by VIB and grants of KU Leuven (C16/15/073), FWO (G078117N and SBO-S006617N), Hercules (AKUL/09/037) and SAO-FRA (S#16018; 2017/033). We also acknowledge NIH grant R01 GM24872 (MHM) and R01 NS NS064015 (LSW).



## References

- Allain, J.M., Storm, C., Roux, A., Ben Amar, M., Joanny, J.F., 2004. Fission of a multiphase membrane tube. *Physical review letters* 93, 158104.
- Anitei, M., Hoflack, B., 2011. Bridging membrane and cytoskeleton dynamics in the secretory and endocytic pathways. *Nat Cell Biol* 14, 11-19.
- Atiba-Davies, M., Noben-Trauth, K., 2007. TRPML3 and hearing loss in the varitint-waddler mouse. *Biochimica et biophysica acta* 1772, 1028-1031.
- Balklava, Z., Niehage, C., Currinn, H., Mellor, L., Guscott, B., Poulin, G., Hoflack, B., Wassmer, T., 2015. The Amyloid Precursor Protein Controls PIKfyve Function. *PLoS One* 10, e0130485.
- Baulac, S., Lenk, G.M., Dufresnois, B., Ouled Amar Bencheikh, B., Couarch, P., Renard, J., Larson, P.A., Ferguson, C.J., Noe, E., Poirier, K., Hubans, C., Ferreira, S., Guerrini, R., Ouazzani, R., El Hachimi, K.H., Meisler, M.H., Leguern, E., 2014. Role of the phosphoinositide phosphatase FIG4 gene in familial epilepsy with polymicrogyria. *Neurology* 82, 1068-1075.
- Bellono, N.W., Escobar, I.E., Oancea, E., 2016. A melanosomal two-pore sodium channel regulates pigmentation. *Scientific reports* 6, 26570.
- Berson, J.F., Harper, D.C., Tenza, D., Raposo, G., Marks, M.S., 2001. Pmel17 initiates premelanosome morphogenesis within multivesicular bodies. *Mol Biol Cell* 12, 3451-3464.
- Berson, J.F., Theos, A.C., Harper, D.C., Tenza, D., Raposo, G., Marks, M.S., 2003. Proprotein convertase cleavage liberates a fibrillogenic fragment of a resident glycoprotein to initiate melanosome biogenesis. *J Cell Biol* 161, 521-533.
- Bissig, C., Hurbain, I., Raposo, G., van Niel, G., 2017. PIKfyve activity regulates reformation of terminal storage lysosomes from endolysosomes. *Traffic*.
- Bissig, C., Rochin, L., van Niel, G., 2016. PMEL Amyloid Fibril Formation: The Bright Steps of Pigmentation. *Int J Mol Sci* 17.
- Bonangelino, C.J., Nau, J.J., Duex, J.E., Brinkman, M., Wurmser, A.E., Gary, J.D., Emr, S.D., Weisman, L.S., 2002. Osmotic stress-induced increase of phosphatidylinositol 3,5-bisphosphate requires Vac14p, an activator of the lipid kinase Fab1p. *J Cell Biol* 156, 1015-1028.
- Bright, N.A., Gratian, M.J., Luzio, J.P., 2005. Endocytic delivery to lysosomes mediated by concurrent fusion and kissing events in living cells. *Curr Biol* 15, 360-365.
- Campeau, P.M., Lenk, G.M., Lu, J.T., Bae, Y., Burrage, L., Turnpenny, P., Roman Corona-Rivera, J., Morandi, L., Mora, M., Reutter, H., Vulto-van Silfhout, A.T., Faivre, L., Haan, E., Gibbs, R.A., Meisler, M.H., Lee, B.H., 2013. Yunis-Varon syndrome is caused by mutations in FIG4, encoding a phosphoinositide phosphatase. *American journal of human genetics* 92, 781-791.
- Carlton, J., Bujny, M., Peter, B.J., Oorschot, V.M., Rutherford, A., Mellor, H., Klumperman, J., McMahon, H.T., Cullen, P.J., 2004. Sorting nexin-1 mediates tubular endosome-to-TGN transport through coincidence sensing of high-curvature membranes and 3-phosphoinositides. *Curr Biol* 14, 1791-1800.
- Chow, C.Y., Zhang, Y., Dowling, J.J., Jin, N., Adamska, M., Shiga, K., Szigeti, K., Shy, M.E., Li, J., Zhang, X., Lupski, J.R., Weisman, L.S., Meisler, M.H., 2007. Mutation of FIG4 causes neurodegeneration in the pale tremor mouse and patients with CMT4J. *Nature* 448, 68-72.
- Currinn, H., Guscott, B., Balklava, Z., Rothnie, A., Wassmer, T., 2016. APP controls the formation of PI(3,5)P-2 vesicles through its binding of the PIKfyve complex. *Cell Mol Life Sci* 73, 393-408.

- de Lartigue, J., Polson, H., Feldman, M., Shokat, K., Tooze, S.A., Urbe, S., Clague, M.J., 2009. PIKfyve regulation of endosome-linked pathways. *Traffic* 10, 883-893.
- Delevoeye, C., Heiligenstein, X., Ripoll, L., Gilles-Marsens, F., Dennis, M.K., Linares, R.A., Derman, L., Gokhale, A., Morel, E., Faundez, V., Marks, M.S., Raposo, G., 2016. BLOC-1 Brings Together the Actin and Microtubule Cytoskeletons to Generate Recycling Endosomes. *Current Biology* 26, 1-13.
- Dennis, M.K., Delevoeye, C., Acosta-Ruiz, A., Hurbain, I., Romao, M., Hesketh, G.G., Goff, P.S., Sviderskaya, E.V., Bennett, D.C., Luzio, J.P., Galli, T., Owen, D.J., Raposo, G., Marks, M.S., 2016. BLOC-1 and BLOC-3 regulate VAMP7 cycling to and from melanosomes via distinct tubular transport carriers. *J Cell Biol* 214, 293-308.
- Derivery, E., Sousa, C., Gautier, J.J., Lombard, B., Loew, D., Gautreau, A., 2009. The Arp2/3 activator WASH controls the fission of endosomes through a large multiprotein complex. *Developmental cell* 17, 712-723.
- Di Palma, F., Belyantseva, I.A., Kim, H.J., Vogt, T.F., Kachar, B., Noben-Trauth, K., 2002. Mutations in *Mcoln3* associated with deafness and pigmentation defects in varint-waddler (*Va*) mice. *Proc Natl Acad Sci U S A* 99, 14994-14999.
- Dong, X.P., Shen, D., Wang, X., Dawson, T., Li, X., Zhang, Q., Cheng, X., Zhang, Y., Weisman, L.S., Delling, M., Xu, H., 2010. PI(3,5)P(2) controls membrane trafficking by direct activation of mucolipin Ca(2+) release channels in the endolysosome. *Nature communications* 1, 38.
- Dove, S.K., McEwen, R.K., Mayes, A., Hughes, D.C., Beggs, J.D., Michell, R.H., 2002. Vac14 controls PtdIns(3,5)P(2) synthesis and Fab1-dependent protein trafficking to the multivesicular body. *Curr Biol* 12, 885-893.
- Duex, J.E., Nau, J.J., Kauffman, E.J., Weisman, L.S., 2006a. Phosphoinositide 5-phosphatase Fig 4p is required for both acute rise and subsequent fall in stress-induced phosphatidylinositol 3,5-bisphosphate levels. *Eukaryot Cell* 5, 723-731.
- Duex, J.E., Tang, F., Weisman, L.S., 2006b. The Vac14p-Fig4p complex acts independently of Vac7p and couples PI3,5P2 synthesis and turnover. *J Cell Biol* 172, 693-704.
- Dunn, L.C., and Thigpen, L.W., 1930. The silver mouse: a recessive color variation. *J. Heredity*, 495-498.
- Ferguson, C.J., Lenk, G.M., Meisler, M.H., 2009. Defective autophagy in neurons and astrocytes from mice deficient in PI(3,5)P2. *Hum Mol Genet* 18, 4868-4878.
- Fowler, D.M., Koulov, A.V., Alory-Jost, C., Marks, M.S., Balch, W.E., Kelly, J.W., 2006. Functional amyloid formation within mammalian tissue. *PLoS Biol* 4, e6.
- Gillooly, D.J., Morrow, I.C., Lindsay, M., Gould, R., Bryant, N.J., Gaullier, J.M., Parton, R.G., Stenmark, H., 2000. Localization of phosphatidylinositol 3-phosphate in yeast and mammalian cells. *EMBO J* 19, 4577-4588.
- Giordano, F., Bonetti, C., Surace, E.M., Marigo, V., Raposo, G., 2009. The ocular albinism type 1 (OA1) G-protein-coupled receptor functions with MART-1 at early stages of melanogenesis to control melanosome identity and composition. *Hum Mol Genet* 18, 4530-4545.
- Gopaldass, N., Fauvet, B., Lashuel, H., Roux, A., Mayer, A., 2017. Membrane scission driven by the PROPPIN Atg18. *Embo j* 36, 3274-3291.
- Hellstrom, A.R., Watt, B., Fard, S.S., Tenza, D., Mannstrom, P., Narfstrom, K., Ekesten, B., Ito, S., Wakamatsu, K., Larsson, J., Ulfendahl, M., Kullander, K.,

- Raposo, G., Kerje, S., Hallbook, F., Marks, M.S., Andersson, L., 2011. Inactivation of Pmel alters melanosome shape but has only a subtle effect on visible pigmentation. *PLoS Genet* 7, e1002285.
- Ho, C.Y., Choy, C.H., Wattson, C.A., Johnson, D.E., Botelho, R.J., 2015. The Fab1/PIKfyve phosphoinositide phosphate kinase is not necessary to maintain the pH of lysosomes and of the yeast vacuole. *J Biol Chem* 290, 9919-9928.
- Ho, H., Kapadia, R., Al-Tahan, S., Ahmad, S., Ganesan, A.K., 2011. WIP1 coordinates melanogenic gene transcription and melanosome formation via TORC1 inhibition. *J Biol Chem* 286, 12509-12523.
- Ho, T., Watt, B., Spruce, L.A., Seeholzer, S.H., Marks, M.S., 2016. The Kringle-like Domain Facilitates Post-endoplasmic Reticulum Changes to Premelanosome Protein (PMEL) Oligomerization and Disulfide Bond Configuration and Promotes Amyloid Formation. *J Biol Chem* 291, 3595-3612.
- Hong, N.H., Qi, A., Weaver, A.M., 2015. PI(3,5)P2 controls endosomal branched actin dynamics by regulating cortactin-actin interactions. *J Cell Biol* 210, 753-769.
- Hurbain, I., Geerts, W.J., Boudier, T., Marco, S., Verkleij, A.J., Marks, M.S., Raposo, G., 2008. Electron tomography of early melanosomes: implications for melanogenesis and the generation of fibrillar amyloid sheets. *Proc Natl Acad Sci U S A* 105, 19726-19731.
- Ikonomov, O.C., Sbrissa, D., Fenner, H., Shisheva, A., 2009. PIKfyve-ArPIKfyve-Sac3 core complex: contact sites and their consequence for Sac3 phosphatase activity and endocytic membrane homeostasis. *J Biol Chem* 284, 35794-35806.
- Incerti, B., Cortese, K., Pizzigoni, A., Surace, E.M., Varani, S., Coppola, M., Jeffery, G., Seeliger, M., Jaissle, G., Bennett, D.C., Marigo, V., Schiaffino, M.V., Tacchetti, C., Ballabio, A., 2000. Oa1 knock-out: new insights on the pathogenesis of ocular albinism type 1. *Hum Mol Genet* 9, 2781-2788.
- Jefferies, H.B., Cooke, F.T., Jat, P., Boucheron, C., Koizumi, T., Hayakawa, M., Kaizawa, H., Ohishi, T., Workman, P., Waterfield, M.D., Parker, P.J., 2008. A selective PIKfyve inhibitor blocks PtdIns(3,5)P(2) production and disrupts endomembrane transport and retroviral budding. *EMBO Rep* 9, 164-170.
- Jin, N., Chow, C.Y., Liu, L., Zolov, S.N., Bronson, R., Davisson, M., Petersen, J.L., Zhang, Y., Park, S., Duex, J.E., Goldowitz, D., Meisler, M.H., Weisman, L.S., 2008. VAC14 nucleates a protein complex essential for the acute interconversion of PI3P and PI(3,5)P(2) in yeast and mouse. *EMBO J* 27, 3221-3234.
- Kawaguchi, M., Hozumi, Y., Suzuki, T., 2015. ADAM protease inhibitors reduce melanogenesis by regulating PMEL17 processing in human melanocytes. *J Dermatol Sci* 78, 133-142.
- Lam, A.J., St-Pierre, F., Gong, Y., Marshall, J.D., Cranfill, P.J., Baird, M.A., McKeown, M.R., Wiedenmann, J., Davidson, M.W., Schnitzer, M.J., Tsien, R.Y., Lin, M.Z., 2012. Improving FRET dynamic range with bright green and red fluorescent proteins. *Nat Methods* 9, 1005-1012.
- Lee, Z.H., Hou, L., Moellmann, G., Kuklinska, E., Antol, K., Fraser, M., Halaban, R., Kwon, B.S., 1996. Characterization and subcellular localization of human Pmel 17/silver, a 110-kDa (pre)melanosomal membrane protein associated with 5,6,-dihydroxyindole-2-carboxylic acid (DHICA) converting activity. *The Journal of investigative dermatology* 106, 605-610.
- Lenk, G.M., Ferguson, C.J., Chow, C.Y., Jin, N., Jones, J.M., Grant, A.E., Zolov, S.N., Winters, J.J., Giger, R.J., Dowling, J.J., Weisman, L.S., Meisler, M.H.,

2011. Pathogenic mechanism of the FIG4 mutation responsible for Charcot-Marie-Tooth disease CMT4J. *PLoS Genet* 7, e1002104.
- Lenk, G.M., Szymanska, K., Debska-Vielhaber, G., Rydzanicz, M., Walczak, A., Bekiesinska-Figatowska, M., Vielhaber, S., Hallmann, K., Stawinski, P., Buehring, S., Hsu, D.A., Kunz, W.S., Meisler, M.H., Ploski, R., 2016. Biallelic Mutations of VAC14 in Pediatric-Onset Neurological Disease. *American journal of human genetics* 99, 188-194.
- Leonhardt, R.M., Vigneron, N., Hee, J.S., Graham, M., Cresswell, P., 2013. Critical residues in the PMEL/Pmel17 N-terminus direct the hierarchical assembly of melanosomal fibrils. *Mol Biol Cell* 24, 964-981.
- Leonhardt, R.M., Vigneron, N., Rahner, C., Cresswell, P., 2011. Proprotein convertases process Pmel17 during secretion. *J Biol Chem* 286, 9321-9337.
- Levy, F., Muehlethaler, K., Salvi, S., Peitrequin, A.L., Lindholm, C.K., Cerottini, J.C., Rimoldi, D., 2005. Ubiquitylation of a melanosomal protein by HECT-E3 ligases serves as sorting signal for lysosomal degradation. *Mol Biol Cell* 16, 1777-1787.
- Liggins, M.C., Flesher, J.L., Jahid, S., Vasudeva, P., Eby, V., Takasuga, S., Sasaki, J., Sasaki, T., Boissy, R.E., Ganesan, A.K., 2018. PIKfyve regulates melanosome biogenesis. *PLoS Genet* 14, e1007290.
- Lopes, V.S., Wasmeier, C., Seabra, M.C., Futter, C.E., 2007. Melanosome maturation defect in rab38-deficient retinal pigment epithelium results in instability of immature Melanosomes during transient melanogenesis. *Molecular Biology of the Cell* 18, 3914-3927.
- McCartney, A.J., Zhang, Y., Weisman, L.S., 2014. Phosphatidylinositol 3,5-bisphosphate: low abundance, high significance. *Bioessays* 36, 52-64.
- Peric, A., Annaert, W., 2015. Early etiology of Alzheimer's disease: tipping the balance toward autophagy or endosomal dysfunction? *Acta neuropathologica* 129, 363-381.
- Rajendran, L., Annaert, W., 2012. Membrane trafficking pathways in Alzheimer's disease. *Traffic* 13, 759-770.
- Raposo, G., Tenza, D., Murphy, D.M., Berson, J.F., Marks, M.S., 2001. Distinct protein sorting and localization to premelanosomes, melanosomes, and lysosomes in pigmented melanocytic cells. *J Cell Biol* 152, 809-824.
- Ripoll, L., Heiligenstein, X., Hurbain, I., Domingues, L., Figon, F., Petersen, K.J., Dennis, M.K., Houdusse, A., Marks, M.S., Raposo, G., Delevoye, C., 2018. Myosin VI and branched actin filaments mediate membrane constriction and fission of melanosomal tubule carriers. *J Cell Biol* 217, 2709-2726.
- Rochin, L., Hurbain, I., Serneels, L., Fort, C., Watt, B., Leblanc, P., Marks, M.S., De Strooper, B., Raposo, G., van Niel, G., 2013. BACE2 processes PMEL to form the melanosome amyloid matrix in pigment cells. *Proc Natl Acad Sci U S A* 110, 10658-10663.
- Romer, W., Pontani, L.L., Sorre, B., Rentero, C., Berland, L., Chambon, V., Lamaze, C., Bassereau, P., Sykes, C., Gaus, K., Johannes, L., 2010. Actin dynamics drive membrane reorganization and scission in clathrin-independent endocytosis. *Cell* 140, 540-553.
- Roux, A., Cuvelier, D., Nassoy, P., Prost, J., Bassereau, P., Goud, B., 2005. Role of curvature and phase transition in lipid sorting and fission of membrane tubules. *Embo j* 24, 1537-1545.
- Rowland, A.A., Chitwood, P.J., Phillips, M.J., Voeltz, G.K., 2014. ER contact sites define the position and timing of endosome fission. *Cell* 159, 1027-1041.

- Rudge, S.A., Anderson, D.M., Emr, S.D., 2004. Vacuole size control: regulation of PtdIns(3,5)P<sub>2</sub> levels by the vacuole-associated Vac14-Fig4 complex, a PtdIns(3,5)P<sub>2</sub>-specific phosphatase. *Mol Biol Cell* 15, 24-36.
- Rutherford, A.C., Traer, C., Wassmer, T., Pattni, K., Bujny, M.V., Carlton, J.G., Stenmark, H., Cullen, P.J., 2006. The mammalian phosphatidylinositol 3-phosphate 5-kinase (PIKfyve) regulates endosome-to-TGN retrograde transport. *J Cell Sci* 119, 3944-3957.
- Salas-Cortes, L., Ye, F., Tenza, D., Wilhelm, C., Theos, A., Louvard, D., Raposo, G., Coudrier, E., 2005. Myosin Ib modulates the morphology and the protein transport within multi-vesicular sorting endosomes. *J Cell Sci* 118, 4823-4832.
- Sannerud, R., Esselens, C., Ejsmont, P., Mattera, R., Rochin, L., Tharkeshwar, A.K., De Baets, G., De Wever, V., Habets, R., Baert, V., Vermeire, W., Michiels, C., Groot, A.J., Wouters, R., Dillen, K., Vints, K., Baatsen, P., Munck, S., Derua, R., Waelkens, E., Basi, G.S., Mercken, M., Vooijs, M., Bollen, M., Schymkowitz, J., Rousseau, F., Bonifacino, J.S., Van Niel, G., De Strooper, B., Annaert, W., 2016. Restricted Location of PSEN2/gamma-Secretase Determines Substrate Specificity and Generates an Intracellular Abeta Pool. *Cell* 166, 193-208.
- Sbrissa, D., Ikonov, O.C., Filios, C., Delvecchio, K., Shisheva, A., 2012. Functional dissociation between PIKfyve-synthesized PtdIns5P and PtdIns(3,5)P<sub>2</sub> by means of the PIKfyve inhibitor YM201636. *American journal of physiology. Cell physiology* 303, C436-446.
- Seaman, M.N., Gautreau, A., Billadeau, D.D., 2013. Retromer-mediated endosomal protein sorting: all WASHed up! *Trends in cell biology* 23, 522-528.
- Seiji, M., Fitzpatrick, T.B., Simpson, R.T., Birbeck, M.S., 1963. Chemical composition and terminology of specialized organelles (melanosomes and melanin granules) in mammalian melanocytes. *Nature* 197, 1082-1084.
- Setty, S.R., Tenza, D., Truschel, S.T., Chou, E., Sviderskaya, E.V., Theos, A.C., Lamoreux, M.L., Di Pietro, S.M., Starcevic, M., Bennett, D.C., Dell'Angelica, E.C., Raposo, G., Marks, M.S., 2007. BLOC-1 is required for cargo-specific sorting from vacuolar early endosomes toward lysosome-related organelles. *Mol Biol Cell* 18, 768-780.
- Sitaram, A., Dennis, M.K., Chaudhuri, R., De Jesus-Rojas, W., Tenza, D., Setty, S.R., Wood, C.S., Sviderskaya, E.V., Bennett, D.C., Raposo, G., Bonifacino, J.S., Marks, M.S., 2012. Differential recognition of a dileucine-based sorting signal by AP-1 and AP-3 reveals a requirement for both BLOC-1 and AP-3 in delivery of OCA2 to melanosomes. *Mol Biol Cell* 23, 3178-3192.
- Sitaram, A., Marks, M.S., 2012. Mechanisms of protein delivery to melanosomes in pigment cells. *Physiology (Bethesda, Md.)* 27, 85-99.
- Theos, A.C., Berson, J.F., Theos, S.C., Herman, K.E., Harper, D.C., Tenza, D., Sviderskaya, E.V., Lamoreux, M.L., Bennett, D.C., Raposo, G., Marks, M.S., 2006a. Dual loss of ER export and endocytic signals with altered melanosome morphology in the silver mutation of Pmel17. *Mol Biol Cell* 17, 3598-3612.
- Theos, A.C., Truschel, S.T., Tenza, D., Hurbain, I., Harper, D.C., Berson, J.F., Thomas, P.C., Raposo, G., Marks, M.S., 2006b. A luminal domain-dependent pathway for sorting to intraluminal vesicles of multivesicular endosomes involved in organelle morphogenesis. *Developmental cell* 10, 343-354.
- van Niel, G., Bergam, P., Di Cicco, A., Hurbain, I., Lo Cicero, A., Dingli, F., Palmulli, R., Fort, C., Potier, M.C., Schurgers, L.J., Loew, D., Levy, D., Raposo, G., 2015. Apolipoprotein E Regulates Amyloid Formation within Endosomes of Pigment Cells. *Cell Rep* 13, 43-51.

- van Niel, G., Charrin, S., Simoes, S., Romao, M., Rochin, L., Saftig, P., Marks, M.S., Rubinstein, E., Raposo, G., 2011. The tetraspanin CD63 regulates ESCRT-independent and -dependent endosomal sorting during melanogenesis. *Developmental cell* 21, 708-721.
- van Weering, J.R., Verkade, P., Cullen, P.J., 2012. SNX-BAR-mediated endosome tubulation is co-ordinated with endosome maturation. *Traffic* 13, 94-107.
- Viaud, J., Boal, F., Tronchere, H., Gaits-lacovoni, F., Payrastre, B., 2014. Phosphatidylinositol 5-phosphate: a nuclear stress lipid and a tuner of membranes and cytoskeleton dynamics. *Bioessays* 36, 260-272.
- Watt, B., Tenza, D., Lemmon, M.A., Kerje, S., Raposo, G., Andersson, L., Marks, M.S., 2011. Mutations in or near the transmembrane domain alter PMEL amyloid formation from functional to pathogenic. *PLoS Genet* 7, e1002286.
- Watt, B., van Niel, G., Fowler, D.M., Hurbain, I., Luk, K.C., Stayrook, S.E., Lemmon, M.A., Raposo, G., Shorter, J., Kelly, J.W., Marks, M.S., 2009. N-terminal domains elicit formation of functional Pmel17 amyloid fibrils. *J Biol Chem* 284, 35543-35555.
- Zhang, Y., Zolov, S.N., Chow, C.Y., Slutsky, S.G., Richardson, S.C., Piper, R.C., Yang, B., Nau, J.J., Westrick, R.J., Morrison, S.J., Meisler, M.H., Weisman, L.S., 2007. Loss of Vac14, a regulator of the signaling lipid phosphatidylinositol 3,5-bisphosphate, results in neurodegeneration in mice. *Proc Natl Acad Sci U S A* 104, 17518-17523.
- Zolov, S.N., Bridges, D., Zhang, Y., Lee, W.W., Riehle, E., Verma, R., Lenk, G.M., Converso-Baran, K., Weide, T., Albin, R.L., Saltiel, A.R., Meisler, M.H., Russell, M.W., Weisman, L.S., 2012. In vivo, Pikfyve generates PI(3,5)P2, which serves as both a signaling lipid and the major precursor for PI5P. *Proc Natl Acad Sci U S A* 109, 17472-17477.
- Zou, J., Hu, B., Arpag, S., Yan, Q., Hamilton, A., Zeng, Y.S., Vanoye, C.G., Li, J., 2015. Reactivation of Lysosomal Ca<sup>2+</sup> Efflux Rescues Abnormal Lysosomal Storage in FIG4-Deficient Cells. *The Journal of neuroscience : the official journal of the Society for Neuroscience* 35, 6801-6812.

## **Figure 1. Interference with the PIKfyve complex affects melanosome morphology and identity**

A-B) EM analysis of epon-embedded RPE of newborn *Vac14*<sup>+/+</sup> and *Vac14*<sup>-/-</sup> mice (A) and *Fig4*<sup>+/+</sup> and *Fig4*<sup>-/-</sup> mice (B). (Scale bar: 2 $\mu$ m). C-E) Quantification of melanosome number per  $\mu$ m<sup>2</sup> RPE (C), melanosome size (D) and the ratio (R) of maximal width and length of melanosomes (E). F) MNT-1 cells were treated with control siRNAs or siRNAs against VAC14, FIG4 and PIKfyve and knock-down efficiencies were analyzed by immunoblotting. Antibodies to tubulin (anti-TUB) were used as equal loading marker. G) MNT-1 cells treated with siRNAs as in F were fixed, permeabilized and immuno-labelled using anti-LAMP1 (red) and anti-PMEL-NKI antibodies (green). DAPI was used to stain nuclei. Insets show magnifications of the boxed regions. (Scale bars: 10  $\mu$ m). H) Quantification of colocalization between LAMP1 and PMEL fluorescence. I) MNT-1 cells treated with control siRNAs or siRNAs against VAC14, FIG4 or PIKfyve were fixed, permeabilized and immuno-labeled using anti-TYRP1 antibody (green) and DAPI (blue) to stain nuclei. Pigmented melanosomes are shown in bright field images. Panels on the right show magnifications of the boxed regions. (Scale bars: 10  $\mu$ m). J) Quantification of melanin content of MNT-1 cells treated with control siRNAs or siRNAs against VAC14, FIG4 or PIKfyve. K) MNT-1 cells treated with control siRNAs or siRNAs against VAC14, FIG4 or PIKfyve were fixed, permeabilized and immuno-labeled using DAPI (blue) to stain nuclei and anti-PMEL (HMB45) antibody (grey) that recognizes PMEL fibrils. (Scale bars: 10  $\mu$ m). L) Quantification of the mean fluorescence intensity per cell normalized to siCTRL. Data are represented as mean  $\pm$  SEM. (See also Figure S1)

**Figure 2. M-alpha fragments accumulate upon interference with PIKfyve function or lysosomal protease activity**

A) Schematic representation of PMEL maturation and proteolytic processing and sorting. PMEL protein domains: signal peptide (SP), N-terminal region (NTR), polycystic kidney disease protein-1-like repeat domain (PKD), repeat domain (RPT), kringle-like domain (KDL), C-terminal fragment (CTF), intracellular domain (ICD). PMEL processing proteases are indicated in red: proprotein convertase (PC), beta-site APP-cleaving enzyme 2 (BACE2) and presenilin 2 (PSEN2). Colored background highlights the intracellular localization of the different PMEL cleavage forms. B) Table of antibodies used in this study summarizing their epitopes and the major PMEL forms they recognize. C-F) MNT-1 cells were treated for 2 h or 24 h with 1.6  $\mu$ M YM201636 (C-D) or with a mixture of protease inhibitors (100  $\mu$ M leupeptin, 10  $\mu$ M pepstatin A and 10  $\mu$ M E-64d) (E-F) and Triton X-100-soluble (C and E) and Triton X-100-insoluble (D and F) lysates were analyzed by immuno-blotting using antibodies against the PMEL C-terminus (anti-PMEL-C), the PMEL N-terminus (anti-PMEL-N), the PMEL RPT domain (anti-PMEL-HMB45), the PMEL PKD domain (anti-PMEL-I51) and Tubulin (anti-TUB) as equal loading marker. The different PMEL fragments are annotated on the right. Stars indicate M-alpha fragments derived from another isoform generated by alternative splicing. Right panels show higher exposures. Data are represented as mean  $\pm$  SEM. (See also Figure S1)

**Figure 3. Stage I melanosomes and endolysosomes transiently interact and exchange content even upon inhibition of PIKfyve activity** A) MNT-1 cells treated for 2 h with 1.6  $\mu$ M YM201636 or DMSO were fixed, permeabilized and immuno-labelled using DAPI (blue) to stain nuclei and anti-PMEL-N (green) and anti-LAMP1 (red) antibodies to label mature PMEL/M-alpha and endolysosomes, respectively. Panels on the right show magnifications of the boxed regions. (Scale bars: 10  $\mu$ m). B-D) Quantification of the mean fluorescence intensity (FI) of anti-PMEL-N signal in LAMP1 compartments (B), of the number of LAMP1 compartments per cell (C) and of the size of LAMP1 compartments (D). E) MNT-1 cells treated for 2 h with 1.6  $\mu$ M YM201636 or DMSO were fixed, permeabilized and immuno-labelled using DAPI (blue) to stain nuclei and anti-PMEL-N (green) and anti-EEA1 (red) antibodies to label mature PMEL/M-alpha and stage I melanosomes, respectively. Panels on the right show magnifications of the boxed regions. (Scale bars: 10  $\mu$ m). F-H) Quantification of the mean fluorescence intensity (FI) of anti-PMEL-N signal in EEA1 compartments (F), of the number of EEA1 compartments per cell (G) and of the size of EEA1 compartments (H). I-J) MNT-1 cells were co-transfected with LAMP1-mRuby2 (red) and 2xFYVE-GFP (green), to mark endolysosomes and stage I melanosomes, respectively. Then cells were treated for 2 h with DMSO (I) or 1.6  $\mu$ M YM201636 (J) and subsequently YM201636 was washed out for 1 h (Figure S3H). Movies were taken at a frame rate of 0.4 s by spinning disc microscopy. The left panels show the first frame of the movies. The right panels show stills of the magnified regions. (Scale bars: 10  $\mu$ m). J) Quantification of the mean duration time of interaction. L-N) Dextran-AF555 (Dex555) (red) was internalized by 4 h pulse and 20 h chase into lysosomes of MNT-1 cells overexpressing 2xFYVE-GFP (localized on stage I melanosomes). Then cells were treated for 2 h with DMSO (L) or 1.6  $\mu$ M YM201636 (N) and movies were taken at a frame rate of 0.4 s by spinning disc microscopy. Upper panels show stills of a movie, where lysosomal DextranAF555 is shown in red and 2xFYVE-GFP localized on stage I melanosomes in green. Lower panels illustrate DextranAF555 transfer from lysosomes to 2xFYVE-GFP compartments. In these panels only lysosomal DextranAF555 is shown in grey and circles indicate the positions of the 2xFYVE-GFP compartment. M-O) Fluorescence intensity of lysosomal DextranAF555 in 2xFYVE-GFP compartments denoted with circles in L and N in cells treated with DMSO (M) and YM201636 (O). Data are represented as mean  $\pm$  SEM. (See also Figure S3)



#### **Figure 4. PMEL fragments accumulate in enlarged EEA1 compartments**

A-B) EM analysis of epon-embedded MNT-1 cells treated for 2 h with the PIKfyve inhibitor YM201636 (A) or knocked-down for VAC14, FIG4 and PIKfyve (B). Upper panels show low magnification overviews of unpigmented and pigmented melanosomes and lower panels show unpigmented melanosomes at higher magnification. Arrowheads point towards enlarged stage I melanosomes and arrows highlight aberrant unpigmented melanosomes containing unstructured aggregates present in VAC14, FIG4 and PIKfyve knock-down cells. (Scale bars: upper panels 500 nm and lower panels 200 nm). C) Quantification of stage I melanosome size. D) Quantification of unpigmented melanosomes grouped into stage I, stage II and aberrant melanosomes. E) Quantification of pigmented and unpigmented melanosomes expressed as a percentage of the total number of melanosomes. F) EM analysis of epon-embedded human primary melanocytes treated with control siRNAs or siRNAs against VAC14, FIG4 and PIKfyve. Right panels show magnifications of stage I melanosomes. (Scale bars: left panels 1  $\mu$ m and right panels 500 nm). G) Ultrathin cryosections of MNT-1 cells treated for 2 h with 1.6  $\mu$ M YM201636 or DMSO were immunogold labelled using anti-PMEL-N antibody followed by protein-A gold 15 nm diameter. Arrows indicate clathrin coats. (Scale bars: 200nm). H) Quantification of the percentage of gold particles on ILVs expressed as a percentage of the total number of gold particles. I) Quantification of the number of gold particles on ILVs per compartment. Data are represented as mean  $\pm$  SEM.

**Figure 5. PIKfyve activity promotes formation of membrane tubules that modulate PMEL accumulation.**

A) Snapshots of live 2xFYVE-GFP transfected MNT-1 cells treated for 2 h with 1.6  $\mu$ M YM201636 or DMSO. Magnifications of the boxed regions illustrate the absence of membrane tubules in PIKfyve inhibitor treated cells. (Scale bars: 10  $\mu$ m). B-D) Quantification of 2xFYVE-GFP tubules per cell (B), of 2xFYVE-GFP compartments size (C) and number per cell (D). E) EM analysis of HPF/freeze substituted MNT-1 cells treated for 2 h with DMSO or 1.6  $\mu$ M YM201636 and subsequently YM201636 was washed out for 4 h. Arrows point at membrane tubules and deformations. (Scale bars: 500 nm). F) Examples of compartments undergoing membrane remodeling upon 4h of YM201636 washout. (Scale bars: 200 nm). G-H) Quantification of the percentage of tubulated stage I melanosomes G) and of stage I melanosome size H). Data are represented as mean  $\pm$  SEM. I) MNT-1 cells treated as indicated were fixed, permeabilized and immuno-labelled using DAPI (blue) to stain nuclei and anti-PMEL-N (green) and anti-EEA1 (red) antibodies to label the PMEL/M-alpha and stage I melanosomes, respectively. Panels on the right show magnifications of the boxed regions. (Scale bars: 10  $\mu$ m). J-K) Quantification of EEA1 size (J) and the mean fluorescence (FI) of PMELN in EEA1 compartment (K). Data are represented as mean  $\pm$  SEM.

### **Figure 6. Endosomal actin dynamics is required for membrane tubule release**

A) MNT-1 cells treated for 2 h with DMSO or 1.6  $\mu$ M YM201636 in the presence or absence of 200  $\mu$ M CK-666 were fixed, permeabilized and immuno-labelled using anti-EEA1 antibody (green) and phalloidin-TRITC (red) to label actin. Lower panels show magnifications of the boxed regions. B) Snapshots of live 2xFYVE-GFP expressing MNT-1 cells treated for 2 h with DMSO or 200  $\mu$ M CK-666 and after washout of YM201636 in the absence and presence of 200  $\mu$ M CK-666. Arrows highlight membrane tubules or buds. Magnifications of boxed regions illustrate membrane tubules. C) Stills of compartments of cells in B illustrating membrane tubules and release. White arrows highlight membrane tubules or buds. Green and red arrows highlight membrane bud release and retraction, respectively. D-E) Quantification of tubules per cell (D) and of the percentage of tubules undergoing release (E). F) EM analysis of HPF/freeze substituted MNT-1 cells treated for 2 h 200  $\mu$ M CK-666 or 1.6  $\mu$ M YM201636, which was subsequently washed out for 1 h and 4 h in the presence of 200  $\mu$ M CK-666. Arrows point at membrane tubules and deformations. (Scale bars: 200 nm). G) MNT-1 cells treated as indicated were fixed, permeabilized and immuno-labelled using DAPI (blue) to stain nuclei and anti-PMELN (green) and anti-EEA1 (red) antibodies to label the PMEL/M-alpha and stage I melanosomes, respectively. Panels on the right show magnifications of the boxed regions. (Scale bars: 10  $\mu$ m). H-I) Quantification of EEA1 size (H) and the mean fluorescence (FI) of PMELN in EEA1 compartment (I). Data are represented as mean  $\pm$  SEM.

### **Figure 7. Working model of PIKfyve function in melanosome biogenesis**

Stage I melanosomes are highly dynamic organelles undergoing frequent homotypic fusion and fission. In these compartments PMEL fibril formation is initiated by PMEL processing and sorting to ILVs. PMEL is processed by lysosomal proteases that are delivered to stage I melanosomes via transient interorganelle interactions. PI(3,5)P<sub>2</sub> synthesized by PIKfyve regulates morphology, size and number of stage I melanosomes by promoting formation of membrane tubules and buds that are released in a mechanism involving branched endosomal actin dynamics. Inhibition of PIKfyve activity abrogates membrane remodeling, reduces the number and increases the size of stage I melanosomes leading to accumulation and unstructured aggregation of PMEL thus impairing fibril formation and melanosome maturation. PIKfyve inhibition also prolongs interactions between stage I melanosomes and lysosomes, probably because PIKfyve activity and PI(3,5)P<sub>2</sub> are also involved in membrane remodeling processes that lead to segregation of the two compartments. Prolonged interorganelle interactions most likely cause mislocalization of endolysosomal proteins to melanosomes and a loss of melanosomal identity during the whole melanogenesis process. Inset: schematic representation of the role of PIKfyve activity on the regulation of import/export processes in stage I melanosomes.

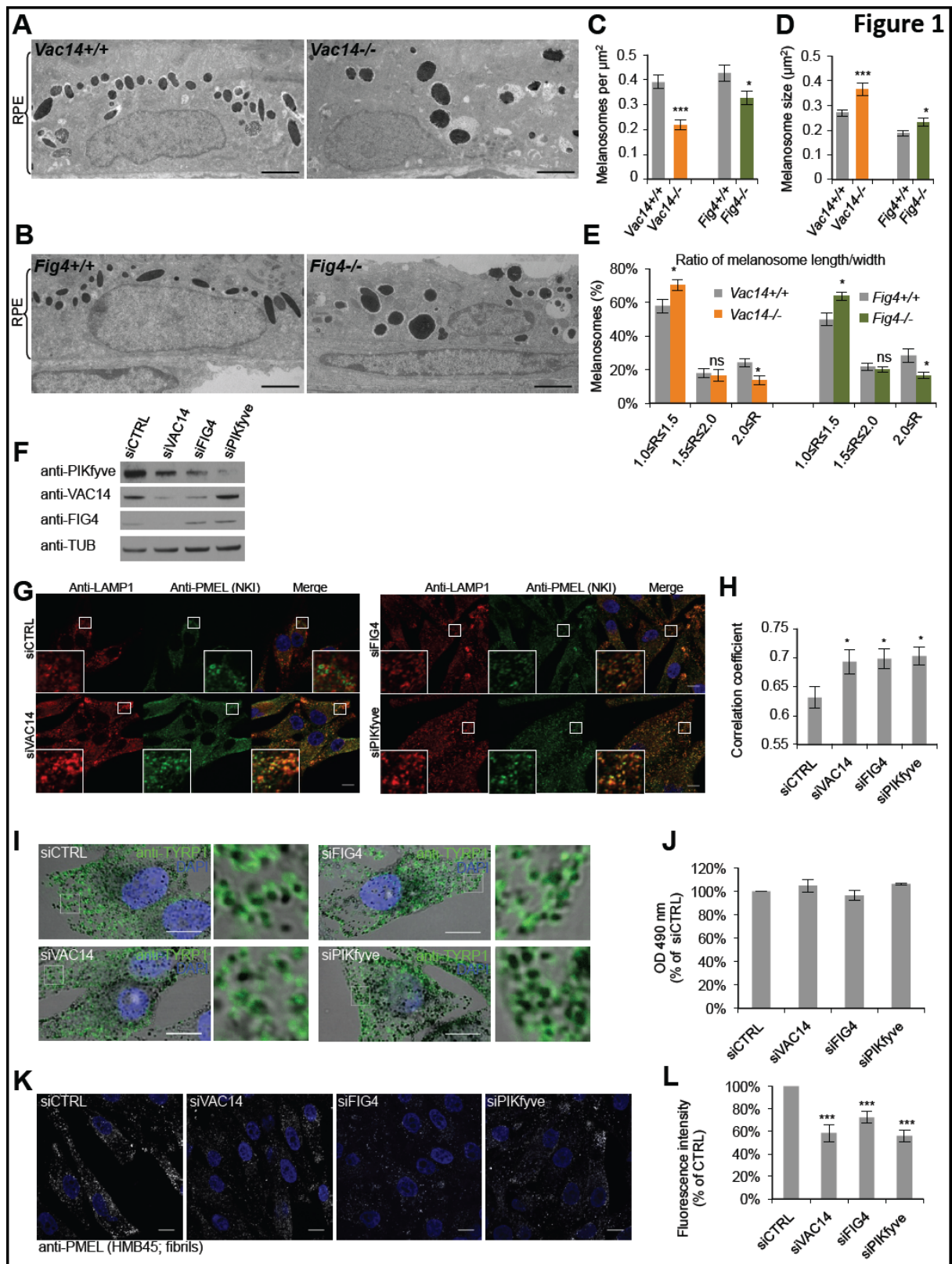
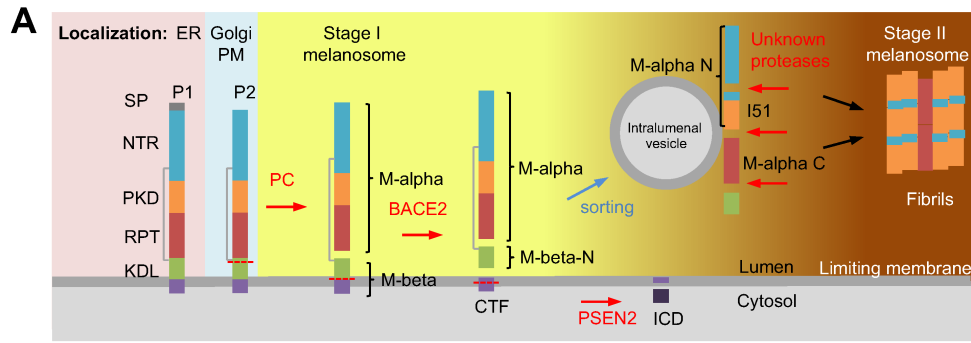
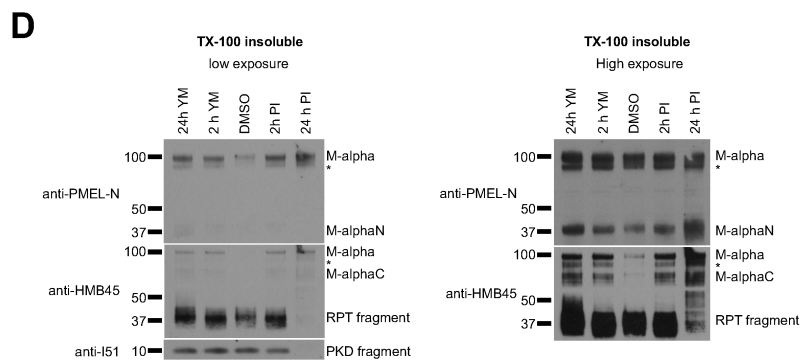
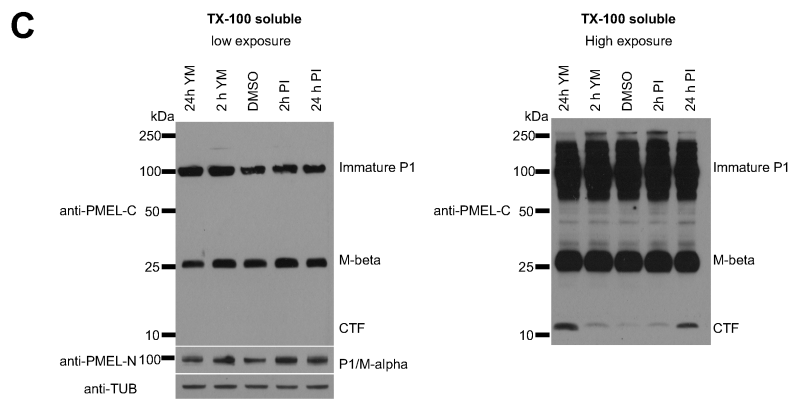


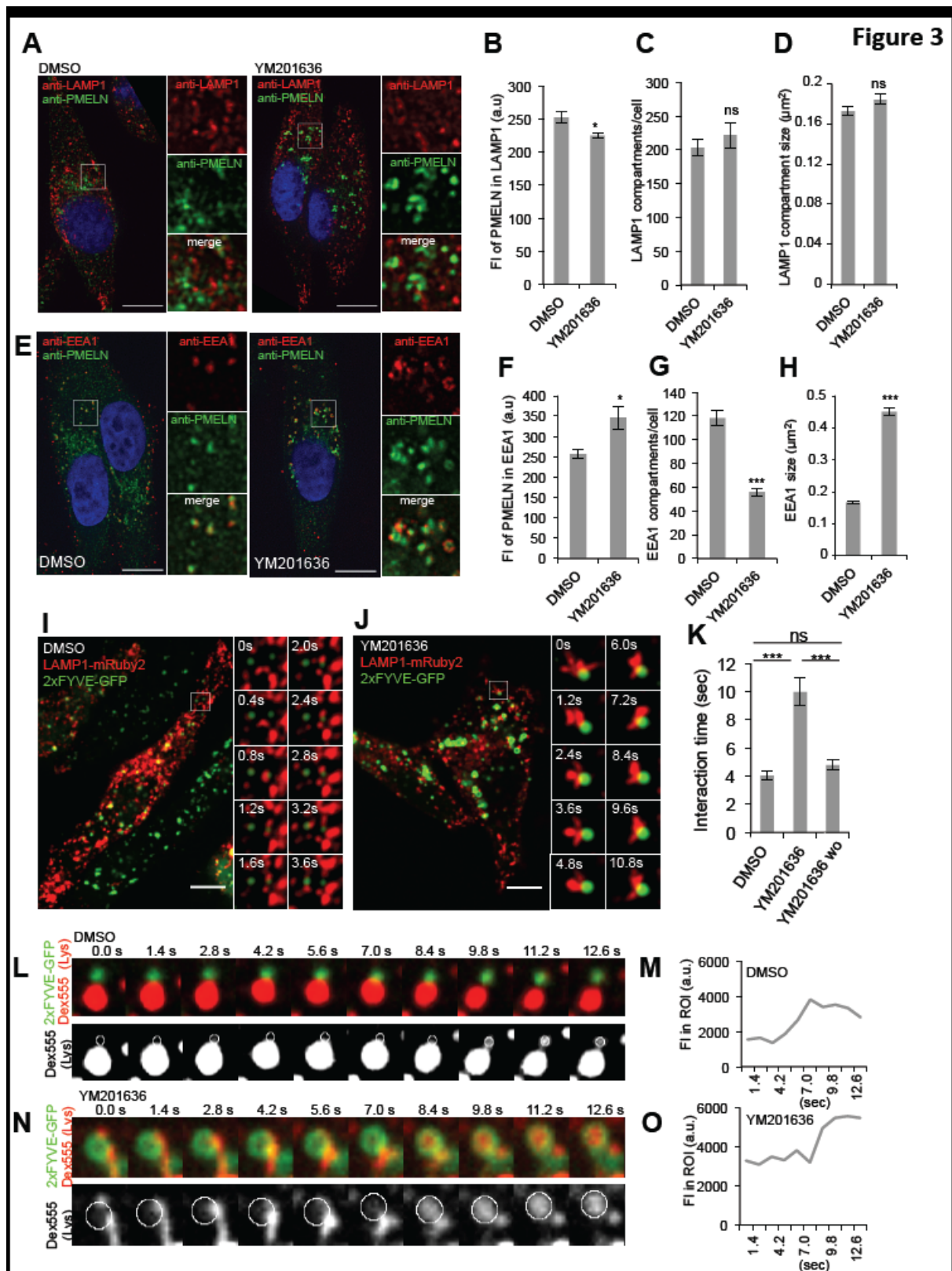
Figure 2



**B**

Antibody	Epitope	Major PMEL form recognized
anti-PMEL-N	PMEL N-terminus	Mature P2, M-alpha, M-alphaN
anti-PMEL-C	PMEL C-terminus	Immature P1, M-beta, CTF
anti-PMEL-NKI	Luminal epitope (PKD)	Processed PMEL in stage II
anti-PMEL-HMB45	Luminal epitope (RPT)	PMEL fibrils, RPT fragment
anti-PMEL-I51	aa 206-220	NTR/PKD fragment





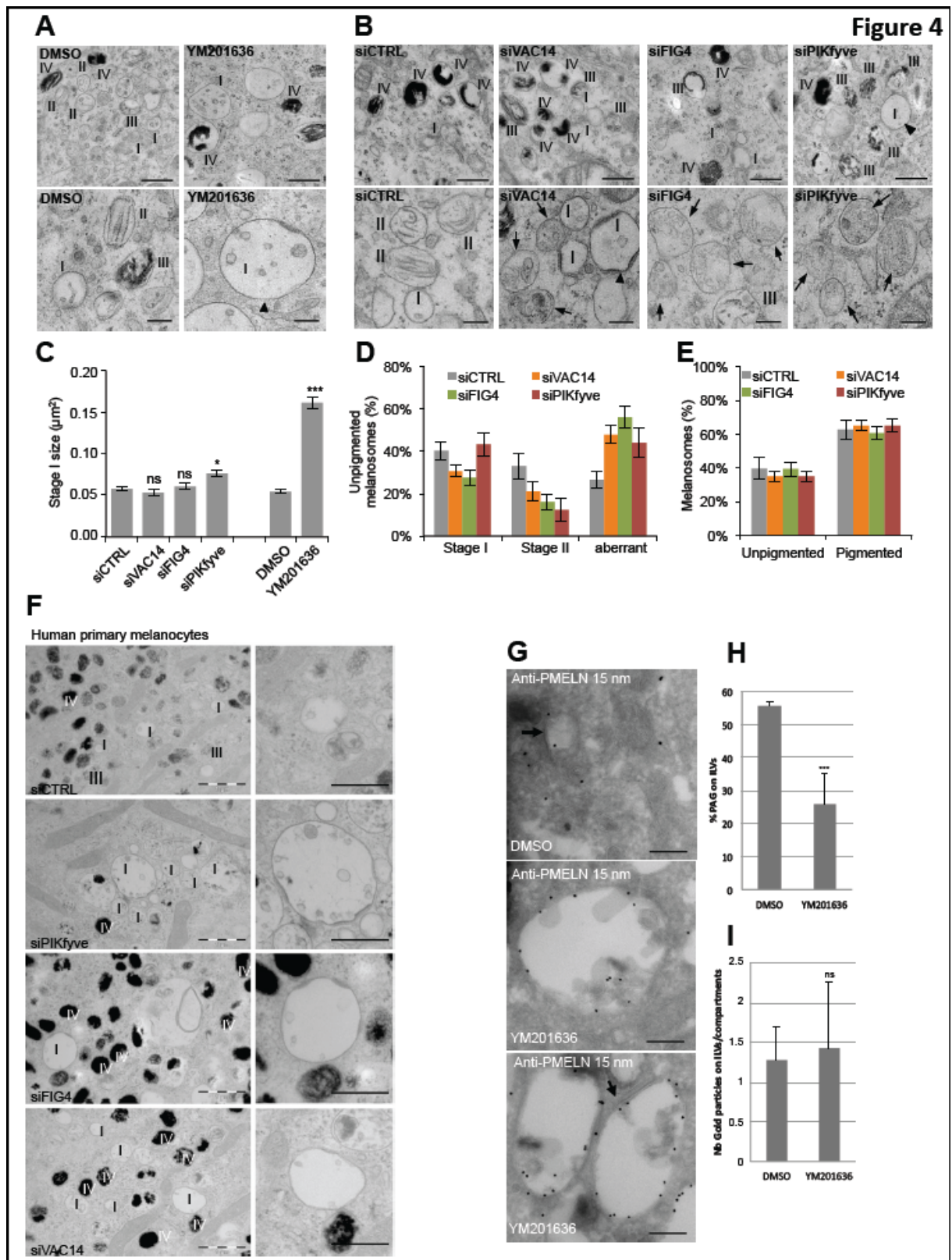
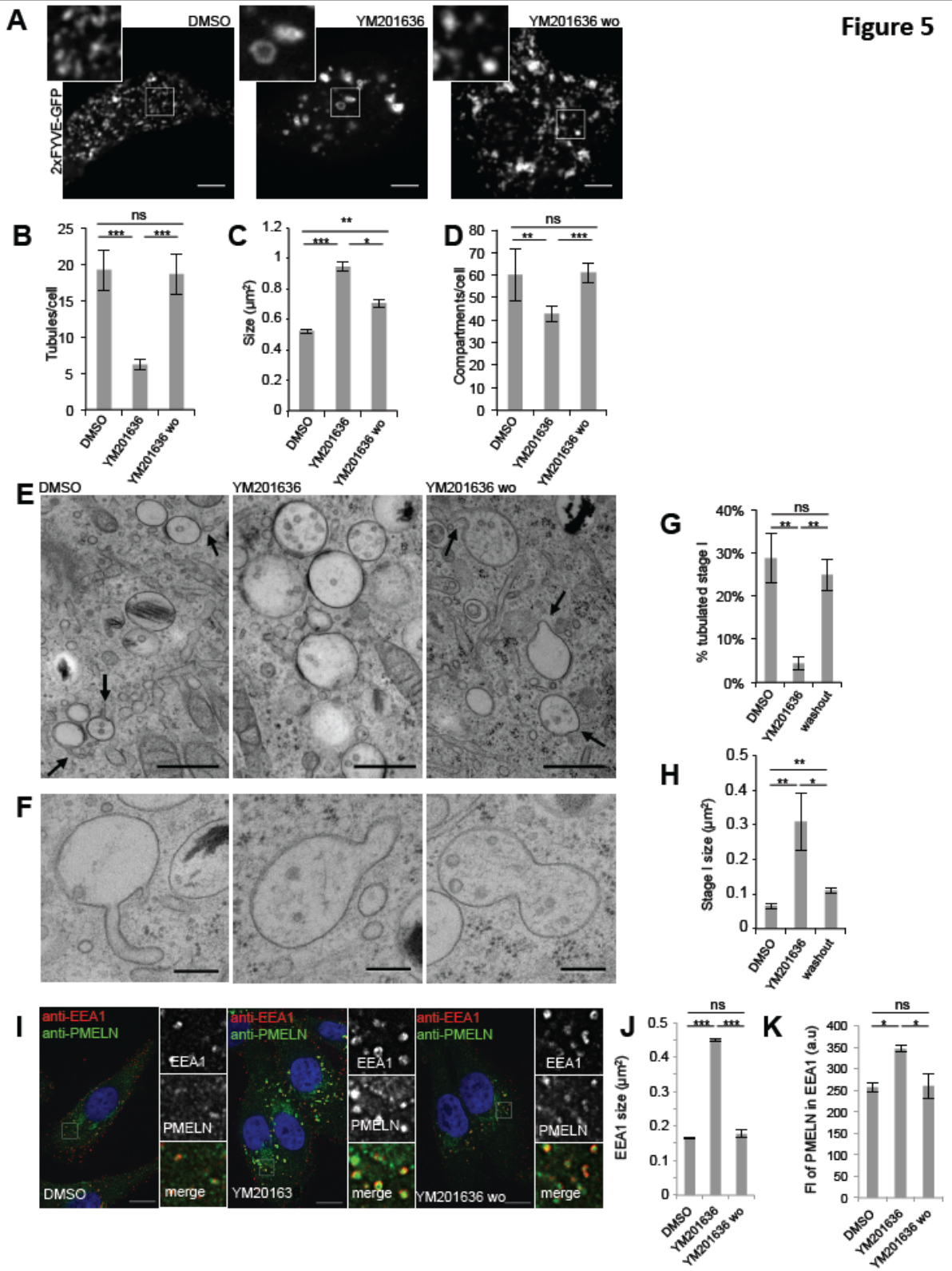


Figure 5



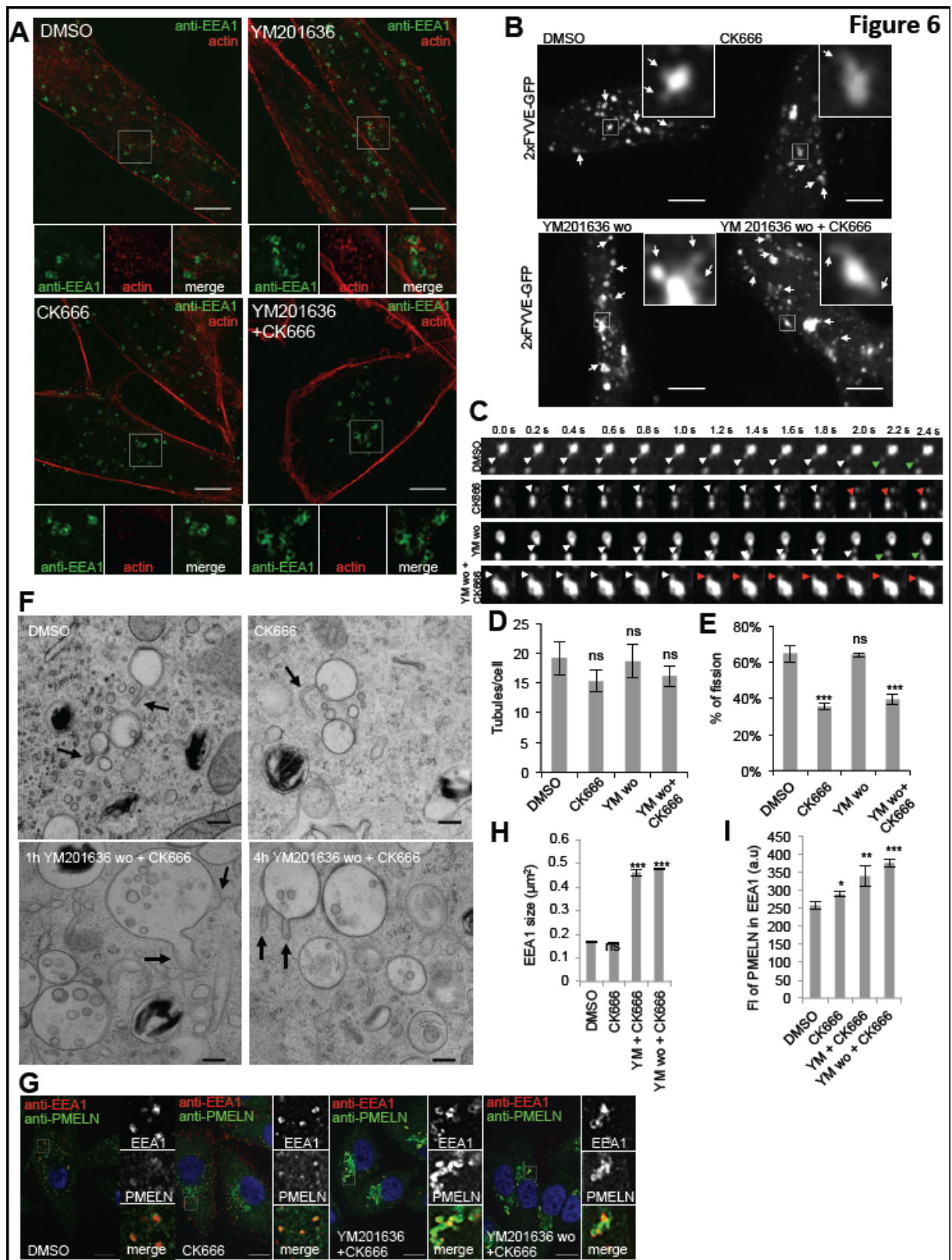




Figure 7

